Published in final edited form as:

Biochim Biophys Acta Mol Basis Dis. 2019 June 01; 1865(6): 1436–1450. doi:10.1016/j.bbadis.2019.02.016.

Mitochondrial and calcium perturbations in rat CNS neurons induce calpain-cleavage of Parkin: Phosphatase inhibition stabilizes pSer^{65}Parkin reducing its calpain-cleavage

Hu Wang[*], **Fanny Cheung**[*], **Anna C. Stoll**, **Patricia Rockwell**, and **Maria E. Figueiredo-Pereira**

Department of Biological Sciences, Hunter College and Graduate Center, City University of New York, NY 10065, USA

Abstract

Mitochondrial impairment and calcium (Ca^{++}) dyshomeostasis are associated with Parkinson's disease (PD). When intracellular ATP levels are lowered, Ca^{++}-ATPase pumps are impaired causing cytoplasmic Ca^{++} to be elevated and calpain activation. Little is known about the effect of calpain activation on Parkin integrity. To address this gap, we examined the effects of mitochondrial inhibitors [oligomycin (Oligo), antimycin and rotenone] on endogenous Parkin integrity in rat midbrain and cerebral cortical cultures. All drugs induced calpain-cleavage of Parkin to ~36.9/43.6 kDa fragments. In contrast, treatment with the proinflammatory prostaglandin J2 (PGJ2) and the proteasome inhibitor epoxomicin induced caspase-cleavage of Parkin to fragments of a different size, previously shown by others to be triggered by apoptosis. Calpain-cleaved Parkin was enriched in neuronal mitochondrial fractions. Pre-treatment with the phosphatase inhibitor okadaic acid prior to Oligo-treatment, stabilized full-length Parkin phosphorylated at Ser^{65}, and reduced calpain-cleavage of Parkin. Treatment with the Ca^{++} ionophore A23187, which facilitates Ca^{++} transport across the plasma membrane, mimicked the effect of Oligo by inducing calpain-cleavage of Parkin. Removing extracellular Ca^{++} from the media prevented oligomycin- and ionophore-induced calpain-cleavage of Parkin. Computational analysis predicted that calpain-cleavage of Parkin liberates its UbL domain. The phosphagen cyclocreatine moderately mitigated Parkin cleavage by calpain. Moreover, the pituitary adenylate cyclase activating peptide (PACAP27), which stimulates cAMP production, prevented caspase but not calpain-cleavage of Parkin. Overall, our data support a link between Parkin phosphorylation and its cleavage by calpain. This mechanism reflects the impact of mitochondrial impairment and Ca^{++}-dyshomeostasis on Parkin integrity and could influence PD pathogenesis.

Graphical abstract

To whom correspondence should be addressed: Maria E. Figueiredo-Pereira, Department of Biological Sciences, Hunter College and Graduate Center, City University of New York, 695 Park Ave., New York, NY 10065, USA, Tel.: 212-650-3565; Fax: or 212-772-5227; pereira@genectr.hunter.cuny.edu.

[*]These authors contributed equally to the work

Conflict of interest: None

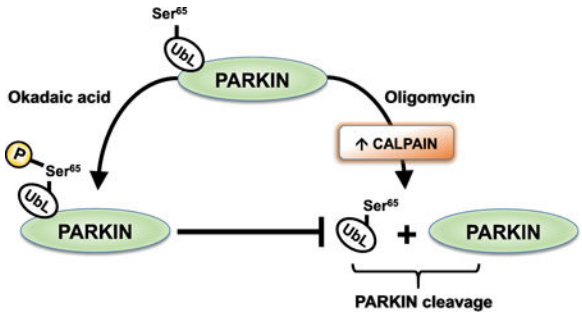

Keywords

Parkin; Mitochondria; Calcium; Calpain; Phosphorylation; Parkinson's disease

1. Introduction

Parkinson's disease (PD) is a multifactorial disorder (Dauer and Przedborski, 2003) in which mitochondrial impairment (Exner et al., 2012;Hauser and Hastings, 2013) and calcium dyshomeostasis (Chan et al., 2009;Zaichick et al., 2017) play a central causative role. Understanding how mitochondrial impairment and calcium dyshomeostasis contribute to the loss of neurons in the nigrostriatal dopaminergic pathway is important for developing neuroprotective therapies that slow or prevent neurodegeneration in PD. To this end, we focused on Parkin, an E3 ubiquitin ligase that is important for proteostasis, mitochondrial homeostasis, and survival of neurons that degenerate in PD. Parkin provides neuroprotection by *(a)* mediating proteasomal-degradation of cytoplasmic proteins, *(b)* targeting some mitochondrial proteins for proteasomal degradation, and *(c)* regulating mitochondrial turnover via mitophagy. Mutations in the *parkin* gene (PARK2) are the most common genetic link to PD (Kumar et al., 2012;Dawson and Dawson, 2010). These mutations act in a loss-of-function manner that impairs the ability of Parkin to ubiquitinate its substrates.

Disruption of Parkin integrity can also account for the loss of its function. Parkin can be cleaved by several proteases. During apoptosis caspase-1, caspase-3 and caspase-8 cleave Parkin at Asp126 resulting in Parkin inactivation (Kahns et al., 2002). The serine protease HtrA2/Omi, which is located in the mitochondrial intermembrane space (Vande et al., 2008), cleaves Parkin between the RING1 and IBR domains also inactivating Parkin (Park et al., 2009). Although Parkin fragments are detected in the substantia nigra of PD patients and Lewy bodies from diseased tissue, the fragments remain to be characterized (Shimura et al., 1999;Schlossmacher et al., 2002). In addition, upon ischemia in mice, Parkin was shown to be rapidly catabolized to unspecified fragments (Mengesdorf et al., 2002). Importantly, Parkin cleavage by calpain has not been investigated.

To address this gap, we compared the effects of oligomycin, epoxomicin and prostaglandin J2 (PGJ2) on Parkin integrity in rat midbrain and cerebral cortical cultures. Oligomycin (Oligo) is a macrolide antibiotic which binds to a polypeptide in the F0 baseplate and blocks ATP synthesis by the F0/F1 mitochondrial ATP synthase (Liu and Schubert, 2009). Epoxomicin (Epox) is a specific and irreversible inhibitor of the proteasome. Epox forms a

covalent adduct with the amino terminal Thr of the 20S proteasome catalytic subunits, generating irreversible morpholino adducts (Meng et al., 1999;Groll et al., 2000). PGJ2 is a product of the cyclooxygenase pathway (Uchida and Shibata, 2008). In rodents, brain levels of PGJ2 are highly induced *in vivo* upon stroke (cerebral ischemia) (Liu et al., 2011a;Liu et al., 2013;Shaik et al., 2014) and traumatic brain injury (TBI) (Kunz et al., 2002;Hickey et al., 2007), reaching concentrations (Shaik et al., 2014) that are neurotoxic. Stroke and TBI increase the long-term risk for PD (Becker et al., 2010;Uchida et al., 2010;Rodriguez-Grande et al., 2013;Hutson et al., 2011;Burke et al., 2013). Recently we were able to mimic in mice and rats various aspects of PD pathology, including neurodegeneration, gliosis, and motor impairment by microinfusing PGJ2 into their substantia nigra (Pierre et al., 2009;Shivers et al., 2014;Corwin et al., 2018). Together, these studies suggest a role for PGJ2 in PD (Figueiredo-Pereira et al., 2015).

When intracellular ATP levels are lowered such as upon Oligo-treatment, Ca^{++}-ATPase pumps are impaired causing cytoplasmic Ca^{++} to be elevated leading to calpain activation (Brini and Carafoli, 2011). Therefore, we also investigated the effect of the calcium ionophore A23187 on Parkin integrity. A23187 increases intracellular calcium levels. The ionophore works mostly by forming stable complexes with divalent cations, which are then able to cross the plasma membrane leading to an increase in the intracellular levels of calcium (Dedkova et al., 2000), thus inducing calpain activation (Chua et al., 2000).

The potential of the pituitary adenylate cyclase activating peptide (PACAP27) was assessed to prevent Parkin cleavage induced by Oligo, Epox and PGJ2. PACAP27 is an endogenous bioactive peptide that is a member of the vasoactive intestinal polypeptide (VIP)-secretin-growth hormone-releasing hormone-glucagon superfamily (Harmar et al., 2012). PACAP was shown to have neuroprotective effects in several *in vivo* and *in vitro* models of neurodegenerative disorders including PD (Reglodi et al., 2011). The neuroprotective effects of PACAP are mediated, in part, by the cAMP/PKA pathway that is known to modulate protein degradation via the UPP (Huang et al., 2013a).

Taking into consideration the structure of Parkin (Wauer and Komander, 2013;Riley et al., 2013;Trempe et al., 2013), our data support the notion that upon mitochondrial impairment or calcium dyshomeostasis or under pro-apoptotic conditions, calpain or caspase-cleavage of Parkin removes its N-terminal ubiquitin-like domain (UbL). Cleavage of the UbL domain of Parkin may prevent its interaction with the 26S proteasome and favor its mitochondrial recruitment to promote mitophagy. Moreover, full-length Parkin phosphorylated at Ser^{65} is less vulnerable to calpain cleavage, while other Parkin phosphorylation sites remain to be assessed. In conclusion, Parkin phosphorylation/dephosphorylation cycle impacts Parkin integrity. Fully understanding its complex regulation and influence on the diverse functions of Parkin, is critical for promoting the survival of neurons that degenerate in PD.

2. Materials and Methods

2.1. Materials –

Inhibitors: oligomycin A (5nM), antimycin A (5nM), and rotenone (20nM to 50nM) were from Sigma-Aldrich (St. Louis, MO); epoxomicin (20nM, Peptides International Inc.,

Louisville, KY); calpeptin (20μM, Z-Leu-Nle-CHO, Calbiochem/EMD Bioscience, Gibbstown, NJ); caspase-3 inhibitor (2μM, Z-DEVD-FMK) and the proteasome substrate Suc-LLVY-AMC (BACHEM Bioscience Inc., King of Prussia, PA); PGJ2 (10μM) and okadaic acid (400nM) were from Cayman Chemical, Ann Arbor, MI). Other drugs: ionophore A23187 (20μM) from Calbiochem, Gibbstown, NJ; PACAP27 (100nM, BACHEM Bioscience Inc., King of Prussia, PA) and cyclocreatine (5mM, Sigma, St. Louis, MO). Primary antibodies: rabbit polyclonal anti-Parkin (1:1000, cat#2132) and anti-caspase-3 (1:1000, cat#9662), as well as mouse monoclonal anti-Parkin (Park8, 1:1000 cat#4211) from Cell Signaling Technology, Danvers, MA; rabbit polyclonal anti-ubiquitinated proteins (1:1,500, cat# Z0458) from Dako North America, Carpinteria, CA; rabbit polyclonal anti-β5 (1:5,000, cat# PW8895) and mouse monoclonal anti-Rpt6 (1:2,000, cat# PW9265) from ENZO Life Sciences, Inc., Farmingdale, NY; mouse monoclonal anti-β-actin (1:10,000, cat# A-2228, from Sigma, St. Louis, MO; mouse monoclonal anti-spectrin α chain (1:5,000. clone AA6, cat# MAB1622) from Millipore, Billerica, MA; mouse monoclonal anti-βIII-tubulin (1:10,000, cat# MMS-435P) from Covance, Oakland, CA; rabbit polyclonal anti-HSP90 (1:2,000, cat# PA3–013) and anti-pSer^{262}Tau (1:20,000, cat#44–750G) from Thermo Fisher Scientific, Rockford, IL; mouse monoclonal Tau C5 (1:50,000; detects all Tau isoforms; epitope, residues 210–241), courtesy of Dr. L. Binder (Northwestern University, Chicago, IL); rabbit polyclonal TOM20 antibody (1:1,000, cat# sc-11415) from Santa Cruz biotechnology Inc, Santa Cruz, CA; mouse monoclonal fibrillarin antibody (1:1,000, cat# ab4566) from Abcam, Cambridge, MA; rabbit polyclonal VDAC antibody (1:1,000, cat# PC548) from Calbiochem, Gibbstown, NJ. The anti-pSer^{65}Parkin rabbit monoclonal antibody was raised by Epitomics (Burlingame, CA) in collaboration with the Michael J Fox Foundation (1:10,000), cat# MJF-17-42-4). Secondary antibodies with HRP conjugate (1:10,000) from Bio-Rad Laboratories, Hercules, CA.

2.2. Primary neuronal cultures –

These studies included two different types of primary neuronal cultures obtained from Sprague Dawley rat embryonic (E18, both sexes) midbrain and cerebral cortical neurons. Midbrain isolation was carried-out as described in (Rayport et al., 1992). Ventral midbrain and cerebral cortical cultures were prepared as we described in (Huang et al., 2013b), details in (Myeku et al., 2011). Cultures were maintained in Neurobasal media supplemented with 2% B27 and 0.5 mM L-Glutamax (all from Invitrogen) at 37°C in a humidified atmosphere containing 5% CO_2. Half of the medium was changed every 4 days. Experiments were run upon 8–11 DIV. According to manufacturer's specifications, Neurobasal medium contains several proprietary factors that ensure a mostly pure (>95%) neuronal culture; glial growth is inhibited without a need for the anti-mitotic agent arabinofuranosyl cytidine (Brewer et al., 1993;Nam et al., 2007).

2.3. Culture treatments –

Neurons were treated (30 min to 16h) with DMSO or with the different drugs in DMSO added directly to DMEM (cat# 11960–044) without serum, supplemented with 0.5 mM L-GlutaMAX and 1 mM sodium pyruvate (all from Invitrogen). In some experiments, cells

were treated in Calcium-free DMEM (cat# 21068–028, Invitrogen). The final DMSO concentration in the medium was 0.5%.

2.4. Mitochondrial fractionation –

Mitochondrial fractionation was carried-out with a mitochondrial isolation kit cat# 89874 (Pierce, Rockford, IL) following the manufacturer's specifications. Four fractions resulted from this procedure: total lysate, crude nuclear, cytosolic and enriched mitochondrial fractions. Protein concentration was determined with the bicinchoninic acid assay (BCA) kit (Pierce, Rockf., IL) for this assay and all others.

2.5. ATP assay –

Steady state ATP content was measured with a kit using the sensitive luciferin/luciferase system (Molecular Probes, Carlsbad, CA) and the Luminoskan Ascent microplate luminometer (Thermo Electron Corporation, Waltham, MA) as previously described (Huang et al., 2013b). ATP levels were normalized for protein concentration.

2.6. Cell viability assay –

Cells were treated under various conditions for 1h to 16h. Cell viability was assessed with the 3-(4,5-dimethylthiazol-2-yl)-2,5-diphenyl tetrazolium bromide (MTT, Mosmann, 1983) assay as previously described (Huang et al., 2013b).

2.7. Western blotting [details in (Myeku et al., 2011)] –

After treatment, cells were rinsed twice with PBS and harvested by gently scraping into hot (100°C) SDS buffer (0.01 M Tris-EDTA, pH 7.5 and 1% SDS) to make sure all intracellular proteins were included. Samples were subjected to a 5min boil at 100°C followed by brief sonication. After determination of the protein concentration the following was added to each sample (final concentrations): β-mercaptoethanol (4%), bromophenol blue (0.005%), and glycerol (4%). Following SDS-PAGE on 6%, 8%, 10% or 12% polyacrylamide gels, proteins were transferred to an Immobilon-P membrane (Millipore, Bedford, MA). The membranes were probed with the respective antibodies and antigens were visualized by a standard chemiluminescent horseradish peroxidase method with the ECL reagent. Semi-quantitative analysis of protein detection was done by densitometry and image analysis with the ImageJ program (Rasband, W.S., ImageJ, U.S. NIH, Maryland, http://rsb.info.nih.gov/ij/, 1997–2006).

2.8. In gel proteasome activity and levels [details in (Myeku et al., 2011)] –

Upon treatment with vehicle (control, DMSO) or the respective drugs, cells were washed twice with PBS and harvested for the in gel assay as described in (Myeku et al., 2011). The native gels loaded with 30 μg protein/lane, were run at 150V for 120min. The in gel proteasome activity was detected by incubating the native gel on a rocker for 10min at 37°C with 15ml of 300μM Suc-LLVY-AMC followed by exposure to UV light (360nm). Gels were photographed with a NIKON Cool Pix 8700 camera with a 3–4219 fluorescent green filter (Peca Products, Inc). Proteins on the native gels were transferred (110mA) for 2h onto PVDF membranes. Immunoblotting was carried-out for detection of the 20S and 26S

proteasomes with the anti-Rpt6 and anti-β5 antibodies, which react with subunits of the 19S or the 20S particles, respectively, thus detecting 26S and 20S proteasomes. Antigens were visualized by a chemiluminescent horseradish peroxidase method with the ECL reagent.

2.9. Caspase-3 and calpain activation –

Cell lysates were analyzed by standard western blotting with the anti-caspase-3 antibody to detect caspase-3 cleavage that is indicative of apoptosis. Calpain activation was assessed with the anti-α-spectrin antibody. Calpain cleavage of α-spectrin generates a 150 kDa doublet, while caspase cleavage generates a 120 kDa fragment.

2.10. Statistical analysis –

Statistical significance was estimated using one or two-way ANOVA (Dunnett's or Tukey's multiple comparison test) or the Student's t-test with the Prism 7 program (GraphPad Software, San Diego, CA).

3. Results

3.1. Oligo, PGJ2, and Epox induce Parkin cleavage in neuronal cultures –

We compared the effects of Oligo, PGJ2 and Epox on Parkin integrity. As shown in Fig. 1 (panels 2), all three drugs induce the cleavage of Parkin in a time-dependent manner. However, the pattern of cleaved Parkin differs among the three drugs. While the size of the Parkin fragment(s) induced by PGJ2 and Epox are below 37 kDa, the ones induced by Oligo are above 37 kDa and appear as a doublet.

The three drugs also differed in relation to their effects on the levels of ubiquitinated proteins, and on activation of caspase-3 and calpain. Oligo induced *(1)* a decrease in the basal levels of ubiquitinated (Ub) proteins (Fig. 1, panel 1), *(2)* calpain activation, indicated by generation of the 150 kDa calpain-specific fragments (Fig. 1, panel 4, α-spectrin CL1), and *(3)* cleavage of caspase-3 to a fragment (~29 kDa) that reflects caspase-3 inactivation (Fig. 1, panel 3). In contrast, PGJ2 and Epox induced *(1)* an increase in Ub-proteins (Fig. 1, panels 1), *(2)* caspase activation, confirmed by generation of the 17 kDa fragment corresponding to activated caspase-3 (Fig. 1, panels 3), and *(3)* formation of the caspase-dependent 120 kDa spectrin fragment. Note that full-length spectrin is only visible in the Epox blot (Fig. 1, panel 4). This blot was exposed for a longer period of time to show the time-dependent formation of the spectrin 120 kDa fragment, detected in the last lane.

Together, these results clearly indicate that PGJ2 and Epox diverge from Oligo on their impact *(1)* on the function of the ubiquitin/proteasome pathway (UPP), in particular on Parkin cleavage and Ub-protein levels, and *(2)* on cell death pathways represented by caspase-3 (apoptosis) or calpain (necrosis) activation.

3.2. Oligo, PGJ2, and Epox induce calpain and caspase-cleavage of Parkin –

It is known that Parkin is a substrate for caspases, as it is cleaved by caspase-1, caspase-3 and caspase-8 at Asp126, leading to its inactivation in Parkin overexpressing CHO and SY5Y cells (Kahns et al., 2002). We now report that in rat midbrain neuronal cultures PGJ2

and Epox induce caspase-3 mediated Parkin cleavage. This is confirmed by inhibition of Parkin-cleavage under these conditions with a caspase-3 specific inhibitor (Z-DEVD-FMK, C3I, Fig. 2B, panel 1) but not by the calpain specific inhibitor calpeptin (CPT, Fig. 2A, panel 1). As expected, caspase-mediated cleavage of α-spectrin (α-spectrin CL2) induced by PGJ2 and Epox, was lessened by the caspase inhibitor.

We also established for the first time to our knowledge, that Parkin is cleaved by calpain upon mitochondrial impairment with Oligo. This cleavage of Parkin is blocked by the calpain inhibitor (CPT, Fig. 2A, panel 1), and is refractory to the caspase inhibitor (C3I, Fig. 2B, panel 1). Calpain-cleaved Parkin migrates at a size that differs from the caspase-cleaved fragments triggered by PGJ2 and Epox (Fig. 2A and B, panels 1). Activation of calpain and caspase and the specificity of the inhibitors for these two proteases are confirmed by the pattern of α-spectrin cleavage shown in Fig. 2A and B, panels 2. It is clear that Oligo induced calpain-cleavage of α-spectrin to a 150 kDa fragment (α-spectrin CL1).

Based on semi-quantitative analysis of the cleaved Parkin doublet compared to full-length Parkin, we estimate that at least 43.6 ± 4.9 % of full-length Parkin is cleaved upon treatment with 5nM Oligo for 16h (n = 9).

3.3. The effect of Oligo on Parkin is mimicked by other mitochondrial inhibitors –

To test if other mitochondrial inhibitors recapitulate the effect of Oligo on Parkin, rat midbrain neuronal cultures were treated with two different mitochondrial toxins that affect different elements of the electron transport chain: *(1)* antimycin A (A5) that binds to the quinone reduction site of complex III (ubiquinol-cytochrome c oxidoreductase), inhibiting the reduction of cytochrome c, and *(2)* rotenone (R) that binds to ND1 and inhibits NADH–ubiquinone reductase activity of complex I (Degli, 1998). Rotenone is particularly relevant to PD, as its effects in *in vivo* models mimic some of the pathological features of PD (Betarbet et al., 2000). We showed previously with rat cortical neurons that oligomycin, antimycin and rotenone reduced the mitochondrial membrane potential ($\Delta\Psi_m$) and increased ROS in addition to decreasing ATP levels (Huang et al., 2013b).

Like Oligo, the two other mitochondrial inhibitors induced calpain-dependent cleavage of Parkin (Fig. 3A, panels 1 and 2). Panel 2 (short exposure) compares the loss of full-length Parkin (parkin FL) caused by each of the drugs. Antimycin and rotenone, like Oligo, also triggered cleavage of caspase-3 to an inactive form (Fig. 3A, panel 3 and 4), and cleavage of α-spectrin (Fig. 3A, panel 5). From the three mitochondrial drugs tested, rotenone caused the weakest changes as it required the highest concentrations to generate detectable levels of calpain-cleaved Parkin by western blot analysis (Fig. 3B). In summary, we show that three mitochondrial toxins that inhibit oxidative phosphorylation at different steps, lead to the generation of calpain-cleaved forms of Parkin. These data support that calpain rather than caspase-3 functions under conditions where ATP levels are limiting. The effect of PGJ2 (J10 in A and J2 in B) are included for comparison.

3.4. Calpain-cleaved Parkin is enriched in neuronal mitochondrial fractions –

We investigated the subcellular localization of cleaved Parkin in rat cerebral cortical cultures treated with Oligo (O5, 5nM), PGJ2 (J10, 10μM), and Epox (E20, 20nM). We performed

these studies with cortical cultures instead of midbrain cultures, because this study requires large numbers of cells that are easily prepared from rat E18 brains. As shown in Fig. 4 (panels 1 & 2), the cortical neurons respond to the three drugs in a manner that is similar to the midbrain cultures. It is clear that full-length (FL) Parkin is detected in nuclear, mitochondrial and cytosolic fractions regardless of cellular conditions, as previously reported in (Van, V et al., 2011). In contrast, most of the calpain-cleaved Parkin (induced by Oligo) fractionates with mitochondria, while caspase-cleaved Parkin (induced by PGJ2 and Epox) is distributed between the nuclear and mitochondrial fractions (Fig. 4, panels 1 & 2). Subcellular markers are: nuclear – fibrillarin (Fig. 4, panels 3 & 4), a nucleolar protein that is regulated by the UPP (Endo et al., 2009); mitochondrial – Tom20 (Fig. 4, panels 5 & 6), a peripheral member of the TOM complex that is the primary receptor for import of mitochondrial precursor proteins (Hachiya et al., 1995), and VDAC (Fig. 4, panels 7 & 8), the voltage-dependent anion channel located on the mitochondrial outer membrane (Shoshan-Barmatz et al., 2010); and cytosolic – Hsp90 (Fig. 4, panels 9 & 10) a well-established chaperone (Bose et al., 1996) also localized to mitochondria (Altieri, 2013).

3.5. Phospho-Parkin is less vulnerable to calpain-cleavage –

Studies with HEK293 and SH-SY5Y cells demonstrated that the turnover of phospho-Parkin is rapid, as treatment with the phosphatase inhibitor okadaic acid (OA) is necessary to stabilize phospho-Parkin (Yamamoto et al., 2005). We confirmed with the rat neuronal cultures that OA stabilizes a Parkin form with a slightly higher molecular weight than full-length Parkin (pSer^{65}parkin FL, Fig. 5, anti-parkin panel, lanes b and d, dashed box). As seen in Fig 5 (anti-pSer^{65} parkin panel, lanes b and d, dashed box), we further established that this higher molecular weight form of Parkin is detected with an antibody developed specifically for pSer^{65} Parkin (pSer^{65} parkin FL). This antibody was raised against a synthetic peptide corresponding to residues surrounding Ser^{65} of human Parkin (Kondapalli et al., 2012). Other potential Parkin phosphorylation sites remain to be assessed. Our data support a transient phospho/dephospho cycle for Parkin FL (Fig. 5, compare lanes a/c with b/d).

Importantly, we also show that pre-treatment with the phosphatase inhibitor OA decreased the susceptibility of full-length Parkin (parkin FL) to calpain-cleavage by as much as 56% (Fig. 5, anti-parkin panel, compare parkin CL in lanes c and d, and the graph). Moreover, it is clear that the calpain-cleaved forms of Parkin (parkin CL) are not detected with the anti-pSer^{65} parkin antibody, suggesting that the UbL domain containing the Ser^{65} of Parkin was removed (Fig. 5, panel 2). The potential calpain-mediated cleavage sites on Parkin are addressed below under “discussion”.

We previously demonstrated that Oligo-treatment of neurons induces calpain-cleavage of other substrates, in particular the microtubule associated protein tau (Huang et al., 2013b). In the current study, we evaluated the levels of total and pSer^{262}tau for comparison with Parkin, as well as cell morphology in neuronal cultures pre-treated with OA prior to Oligo. As expected Oligo-treatment induced cleavage of tau to several fragments (Fig. 5B). OA promoted tau phosphorylation at Ser 262 (Fig. 5B), which accumulates in neurofibrillary tangles in Alzheimer’s disease (AD) brains (Lauckner et al., 2003). Furthermore, OA and

Oligo-treatment separately or in combination altered cell morphology, in particular the neuronal processes, suggesting cytoskeletal disruption (Fig. 5C).

3.6. Calcium dyshomeostasis also induces calpain cleavage of endogenous neuronal Parkin –

Treatment with the Ca^{++} ionophore A23187 (ION, 20μM, 1hour) or Oligo-treatment (5nM, 16hours) induced similar calpain-dependent Parkin cleavage to a doublet with a molecular mass > 37 kDa (Fig. 6A, panel 1). Calpain-activation is depicted by spectrin cleavage to the 150 kDa fragment (Fig. 6A, panel 3). Therefore, we established for the first time to our knowledge, that Parkin is cleaved by calpain upon treatment with the ionophore A23187, which disrupts calcium homeostasis. Calpain-cleaved Parkin was also detected with the mouse monoclonal anti-Parkin (Park8) antibody from Cell Signaling (not shown). The ionophore-induced cleavage of Parkin was blocked by the calpain inhibitor calpeptin (CPT, Fig. 6B, panels 1), as was spectrin cleavage (Fig. 6B, panels 3).

We also addressed whether Oligo- and ION-induced calpain-cleavage of Parkin and spectrin are Ca^{++}-dependent. We incubated (1h) neurons in Ca^{++} free medium prior to exposure to Oligo (6h 30min) or ION (one hour) in the same Ca^{++} free medium (Fig. 6C and 6D, respectively). This protocol was chosen in part since the calcium chelator BAPTA was toxic to neurons under our incubation conditions. To prevent excessive toxicity, the Oligo-treatment was shortened to 6h 30min under Ca^{++} free conditions. We show that calpain-cleavage of Parkin (Fig. 6C and 6D, panels 1) or spectrin (Fig. 6C and 6D, panels 3) are largely eliminated under Ca^{++} free conditions.

Chronic neurodegenerative disorders like PD, are linked to mitochondrial dysfunction, disruption of calcium homeostasis, and accumulation/aggregation of ubiquitinated (Ub) proteins (Oddo, 2008). We compared the effect of the mitochondrial inhibitor Oligo (5nM, 16h) with the ionophore A23187 (ION, 20μM, 1h) on Ub-protein levels in the cortical neurons. Both drugs decreased the basal levels of Ub-protein detected under control conditions (Figure 6A, panel 4).

3.7. Effects of Oligo, PGJ2 and Epox on the proteasome –

These current studies are a continuation of our previous findings with cortical neurons (Huang et al., 2013b) showing that Oligo, antimycin or rotenone trigger 26S proteasome disassembly with a rise in 20S proteasomes.

Therefore, we assessed with the native in-gel assay, the effects of the three drugs on proteasome activity and levels in the midbrain neurons as described in (Huang et al., 2013b). The in-gel assay detects the three assembled forms of the proteasome: 26S proteasomes with either two regulatory caps [26S (2)] or one cap [26S(1)], and the 20S core particle alone (20S). The three drugs decreased 26S proteasome activity with Epox being the most efficient of the three (Fig. 7, panels 1 & 6). Oligo ($p<0.001$) and PGJ2 (did not reach statistical significance) increased 20S proteasome activity (Fig. 7, panels 2 & 6). Oligo (O, 5nM) and PGJ2 (J, 10μM, did not reach statistical significance) also decreased the levels of the 26S proteasome while increasing those of the 20S proteasome (Fig. 7, panels 3, 4 & 7). Epox

however, did not increase 20S proteasome levels. In conclusion, Oligo affects proteasome activity in midbrain cultures replicating the Oligo-effect on cortical neurons.

Previously, we also showed that the mitochondrial inhibitors induce a reduction in basal levels of ubiquitinated proteins due in part to inhibition of the E1A ubiquitin activating enzyme (Huang et al., 2013b). It is thus clear that mitochondrial impairment slows down the ubiquitin/proteasome pathway by: 1) blocking its first step, *i.e.* preventing ubiquitin activation by the E1 enzyme, which is ATP-dependent; 2) provoking the demise of 26S proteasomes in neurons caused by 26S proteasome disassembly. This latter event seems to be linked to selective processing of the proteasome Rpn10 subunit by calpain (Huang et al., 2013b).

3.8. Comparison of the effects of Oligo, PGJ2 and Epox on cell viability and ATP levels –

Since the three drugs act via different mechanisms, we compared their effects on cell viability and ATP levels. At the concentrations and times tested, Oligo (5nM) was the most neurotoxic, decreasing cell viability by ~50%, followed by PGJ2 (10μM, ~20% decrease) and Epox (20nM) less than 4% (not significant), as shown in Fig. 8A. Oligo was the only drug that decreased intracellular ATP levels, causing ~60% depletion (Fig. 8B). Moreover, we previously demonstrated that Oligo-treatment of rat cortical neurons elevated ROS production and decreased $\Delta\Psi_m$ (Huang et al., 2013b), further supporting that Oligo-treatment impairs mitochondrial function. We proposed then that the decline in $\Delta\Psi_m$ caused by long-term oligomycin treatment is consistent with the overall loss of metabolic activity (Huang et al., 2013b).

3.9. PACAP27 and cyclocreatine mitigate some of the effects of PGJ2 and Oligo, respectively –

cAMP-signaling is known to be neuroprotective (Huang et al., 2013a). In particular, we previously established that raising intracellular cAMP levels with the lipophilic peptide PACAP27 prevents the cleavage of TAU, a microtubule associated protein, and caspase-3 activation both induced by PGJ2 in rat cerebral cortical neuronal cultures (Metcalfe et al., 2012). We now demonstrate in rat midbrain cultures (Fig. 9A) that PACAP27 mitigates PGJ2-induced caspase-dependent Parkin cleavage (panel 1), caspase activation (panel 4), and loss in cell viability (panel 5). However, PACAP27 did not cause a decline in the levels of ubiquitinated proteins raised by PGJ2 (Fig. 9A, panel 3).

PACAP27 failed to abolish the Oligo effects that we analyzed in midbrain cultures (data not shown), thus we tested another protective approach. Since Oligo inhibits ATP synthesis by mitochondria, we decided to increase ATP production via a different pathway, i.e. the phosphagen system. We did not consider activating glycolysis, since this approach can increase lactic acid production leading to pH changes. The phosphagen system involves phosphagen kinases, such as creatine kinase, that function to temporally buffer ATP levels in cells, including neurons, that display high and variable rates of aerobic energy production (Ellington, 2001). To activate the creatine phosphate/creatine kinase (CP/CK) phosphagen system we treated rat midbrain cultures with cyclocreatine, as this compound is phosphorylated and dephosphorylated by CKs at the same rate as creatine, but has the

advantage of crossing membranes due to its relatively planar structure (Kurosawa et al., 2012).

We show (Fig. 9B) that cyclocreatine (CCr, 5mM) mitigated the Oligo-induced ATP depletion (panel 6) and calpain-dependent cleavage of Parkin (panel 1) and α-spectrin (panel 4), but did not affect the levels of ubiquitinated proteins (panel 3). Changes in cell viability are not apparent (panel 5), due to the short time of the treatment. In Figure 9, the incubation times with drug differ based on the optimal times needed to see drug effects. In this regard, the effects of CCr is short lived, thus, the 4 hour incubation time in Oligo treated cells.

4. Discussion

In this study we characterize the vulnerability of Parkin integrity to pathological conditions associated with the development of PD. In particular, we address the effects of mitochondrial impairment and calcium dyshomeostasis on endogenous Parkin integrity in rat midbrain and cerebral cortical cultures. Disruption of Parkin integrity via its cleavage by different proteases, blocks its ubiquitination activity (Kahns et al., 2002;Vande et al., 2008;Park et al., 2009), just like Parkin mutations associated with familiar PD.

We demonstrate that calpain-mediated Parkin cleavage is induced by three mitochondrial toxins, Oligo, antimycin and rotenone, and by the Ca^{++} ionophore A23187, which disrupts calcium homeostasis. Our previous studies (Huang et al., 2013b), showed that Oligo, antimycin and rotenone induce a significant decline in ATP levels and $\Delta\Psi_m$, as well as increase ROS production in rat cerebral cortical neurons. Oligo most efficiently depleted ATP levels, followed by antimycin, and rotenone being the least effective. Since Oligo induced the strongest Parkin cleavage and rotenone the weakest, these studies support the notion that changes in ATP levels induced by the three mitochondrial inhibitors correlate with the levels of calpain-mediated Parkin cleavage. Calpain was shown to cleave other proteins highly relevant to PD and other neurodegenerative conditions. Some of these proteins are α-synuclein that becomes aggregation prone upon calpain cleavage (Dufty et al., 2007), 26S proteasome subunit Rpn10 (full-length Rpn10 binds Parkin), Tau and caspase 3 (calpain cleaves caspase 3 to an inactive form) (Huang et al., 2013b), as well as huntingtin (Goffredo et al., 2002).

Although a considerable amount of full-length Parkin is not cleaved, we speculate that it may only take a small fraction of Parkin cleavage by calpain to perturb mitochondrial function. In support of this notion, our subcellular fractionation studies show that cleaved Parkin is localized to the mitochondrial fraction in response to Oligo. We base our premise on previous demonstrations that: 1) Parkin translocates to the mitochondria in response to the mitochondrial stressor CCCP in mouse cortical neurons expressing PINK1 (Joselin et al., 2012), and that 2) Parkin was localized in the mitochondrial fractions of human iPSC-derived neurons and in fibroblasts from PD patients (Hsieh et al., 2016). While our results show that Parkin is partially cleaved in the mitochondrial fraction, it raises the possibility that Parkin function may be sufficiently compromised in response to calpain to affect mitochondrial homeostasis. It is known that Parkin is inactivated by caspase cleavage after Asp 126. Since we predict that calpain-cleavage occurs in the same region, it is possible that

calpain would also inactivate Parkin function. Furthermore, we previously showed (Huang et al., 2013b) that mitochondrial inhibitors induce a reduction in ubiquitinated proteins due in part to inhibition of the E1A ubiquitin activating enzyme, as well as 26S proteasome disassembly with a rise in 20S proteasomes. Together these effects could lead to a toxic accumulation of Parkin substrates and neuronal cell death. Further studies are needed to show whether calpain-cleavage of Parkin perturbs the role of Parkin in maintaining mitochondrial quality control.

Calpain activation is Ca^{++}-dependent. Disruption of Ca^{++} homeostasis is linked to mitochondrial impairment (Cali et al., 2014) and is implicated in the pathogenesis of PD (Zaichick et al., 2017). Ca^{++} concentration in the cytoplasm is 20,000-fold lower than in the extracellular space (Surmeier and Sulzer, 2013). While extracellular Ca^{++} is in the millimolar range, cytosolic Ca^{++} is usually less than one micromolar, except during a Ca^{++} signaling event. Na^{+}/Ca^{++}exchangers and Ca^{++}-ATPase pumps in the plasma and ER membranes maintain this low concentration by transporting Ca^{++} away from the cytoplasm, either out of the cell or into the ER (Schapira, 2013). The dopaminergic neurons (DA) of the substantia nigra pars compacta (SNpc) are particularly sensitive to Ca^{++} dyshomeostasis, because of two main reasons (Rivero-Rios et al., 2014;Surmeier et al., 2017). Firstly, DA neurons of the SNpc have intrinsically low Ca^{++} buffering capacity, compared to DA neurons of the ventral tegmental area (VTA), which express high levels of calbindin, a Ca^{++} buffering protein (Rivero-Rios et al., 2014;Surmeier et al., 2017). Secondly, DA neurons of the SNpc are autonomously active in the absence of synaptic input, by engaging L-type Ca^{++} channels, which cause significant increases in Ca^{++} levels (Rivero-Rios et al., 2014;Surmeier et al., 2017). DA neurons of the VTA also exhibit pacemaker activity, but have significantly lower density of the L-type Ca^{++}channels. Taking these factors into consideration, it is clear that DA neurons of the SNpc are highly vulnerable to Ca^{++} dyshomeostasis, such as caused in our studies by Oligo or ION-treatments. We clearly demonstrate that Oligo- or ION-treatment induce Parkin cleavage in a calcium-dependent manner, thus disrupting Parkin integrity.

Calpains do not have a strict cleavage specificity, although some preferences for particular amino acid sequences, secondary structure (disordered regions) and PEST regions were suggested (Orrenius et al., 2003;Sorimachi and Ono, 2012). To find a putative calpain cleavage site on Parkin, we used two computational programs [http://ccd.biocuckoo.org/ (Liu et al., 2011b) and http://calpain.org (DuVerle et al., 2011)]. These programs predict two calpain cleavage sites (P1 position) in human/rat full-length Parkin (Fig. 10): (1) Gln71 within the following sequence in human: *IVHIV***Q**-*RPWRK* and in rat: *IVHIV***Q**-*RPQRK*, with a predicted molecular weight of 43.6, and located within the UbL domain. (2) Ala134 within the following sequence in human: *KDSPP***A**-*GSPAG* and in rat: *SDSEA***A**-*RGPAA*, with a predicted molecular weight of 36.9, and located within the linker region between the UbL and RING0 domains.

From all reported Parkin alternative splicing variants [reviewed in (Dagata and Cavallaro, 2004)], transcript variant 3 (TV3) lacks exons 3–5 that encode for a.a. 58–206 of full-length Parkin (Mizuno et al., 2003). TV3 has a predicted molecular weight of ~36 kDa (Dagata and Cavallaro, 2004) that is similar to the calpain-cleaved forms of Parkin. However, since the

TV3 form of Parkin is not detected in cells treated with calpain inhibitors, and TV3 lacks the calpain (predicted) cleavage sites, we conclude that the Parkin fragments detected in our studies are cleavage products of full-length Parkin.

In our current studies with rat primary neuronal cultures, we determined that the phosphatase inhibitor okadaic acid stabilized a form of full-length phospho-Parkin. Phospho-Parkin was thus less vulnerable to calpain-cleavage, as the levels of cleaved Parkin were decreased with okadaic acid pre-treatment. One of the calpain-cleavage sites on Parkin that we predicted, Gln71, is in close proximity to one of the Parkin phosphorylation sites, Ser^{65} (Fig. 10). Both sites, Gln71 and Ser^{65}, are located within the UbL domain of Parkin. We found that calpain-cleaved Parkin was not detected with an antibody specific for $pSer^{65}$ within the UbL domain of Parkin. Only full-length phospho-Parkin was detected with this antibody. These data suggest that the UbL domain of Parkin is removed upon calpain cleavage. Others showed that PINK1 phosphorylates Parkin at Ser^{65} (Kondapalli et al., 2012;Shiba-Fukushima et al., 2012), and that this is necessary for maximal Parkin E3-ligase activation (Kazlauskaite et al., 2015). Based on these findings, we propose that stabilization of Parkin phosphorylation at Ser^{65} by phosphatase inhibition attenuates calpain-mediated cleavage of activated Parkin. This phosphorylation-cleavage crosstalk could be a mechanism to prevent long-lasting activation of Parkin.

Studies by others established that Parkin is constitutively phosphorylated at the N- and C-termini, but its phospho/dephospho cycle is rapid as phosphatase inhibitors are necessary to detect phospho-Parkin (Yamamoto et al., 2005). Besides Ser65, two other Parkin phosphorylation sites (Ser131 and Ser136, Fig. 10), were identified in Parkin overexpressing HEK293 and SH-SY5Y cells upon treatment with okadaic acid (Yamamoto et al., 2005). The second calpain-cleavage site we predicted on Parkin, Ala134, is in close proximity to Ser131 and Ser136 (Fig. 10). This suggests that phosphorylation at Ser131 and Ser134, may also protect Parkin from calpain cleavage. Furthermore, since okadaic acid exhibits selectivity for PP2A over PP1, the two most abundant serine/threonine phosphatases in mammalian cells (Boudreau and Hoskin, 2005), it is possible that PP2A activity diminishes Parkin phosphorylation, just as it does for tau hyperphosphorylation (Gong et al., 2000). We show herein that okadaic acid treatment increases the levels of $pSer^{262}$tau, shown to accumulate in tangles in AD brains, and to have a strong disruptive effect on microtubules (Lauckner et al., 2003). Alternatively, at the concentration tested (400nM) okadaic acid could inhibit both PP2A and PP1.

Parkin activation seems to be a multistep event regulated by phosphorylation, cysteine modification, and ligand binding to the UbL domain (Trempe et al., 2013). By mediating protein ubiquitination and by binding to proteasomes, Parkin is able to respond promptly to specific cellular proteolytic requirements involving the UPP. As expected, subcellular fractionation of the neuronal cultures showed that FL-Parkin is located in the cytosolic and mitochondrial fractions. FL-Parkin was also detected in the nuclear fraction. The translocation of Parkin to the nucleus, induced by a range of DNA damaging agents, is thought to play an important role in DNA repair and protect against genotoxicity (Kao, 2009). This is relevant to PD, as oxidative stress induced DNA damage is a potential

pathogenic mechanism implicated in parkinsonism (Migliore et al., 2001;Petrozzi et al., 2001).

In contrast to FL-Parkin, calpain-cleaved Parkin generated upon mitochondrial dysfunction induced by Oligo-treatment, was present only in the mitochondrial fraction. Calpains are located in the cytoplasm, and more recently were found to also be present in mitochondria (Kar et al., 2010). The intracellular location where Parkin is cleaved by calpain and how PINK1 may affect this process remains to be established. Studies by others showed that Parkin associates and regulates the 26S proteasome via binding of the Parkin UbL domain to the Rpn10 subunit of the 26S proteasome (Um et al., 2010;Sakata et al., 2003). Moreover, it is conceivable that the UbL domain alone retains activity and negatively affects proteasome-mediated degradation by competing with other factors for Rpn10 binding (Kahns et al., 2002). In addition, the UbL domain of Parkin seems to delay the translocation of Parkin to mitochondria (Ham et al., 2016). Together, all of these findings support the notion that calpain cleavage liberates the UbL domain of Parkin, thus blocking the Parkin/Rpn10 interaction and freeing Parkin to facilitate mitophagy. This is particularly relevant under conditions of ATP depletion when protein ubiquitination is limited by E1 inhibition as we previously demonstrated (Huang et al., 2013b). Interestingly, the Arg to Pro mutation at position 42 of the UbL domain of Parkin, identified in patients with autosomal-recessive juvenile parkinsonism (ARJP), disrupts the Rpn10-Parkin interaction (Sakata et al., 2003). Thus, disruption of the Rpn10-Parkin interaction due to mutations in Parkin (Um et al., 2010) or to its calpain-cleavage, as we demonstrate here, could mediate disruption of Parkin-26S proteasome interactions, and have an impact on PD pathology.

Based on our data, PGJ2 does not mitigate ATP levels, and increases the levels of ubiquitinated proteins and caspase-mediated Parkin cleavage. PGJ2 is a product of inflammation postulated to activate the Fas/FasL death signaling pathway (Kondo et al., 2002) and caspase-8 (Metcalfe et al., 2012), thus linking inflammation to caspase-mediated loss of Parkin activity and accumulation of its substrates. These effects are replicated by proteasome inhibition with Epox. In contrast, Oligo significantly reduced mitochondrial production of ATP and protein ubiquitination, and leads to calpain-mediated Parkin cleavage. Both of these conditions are associated with PD pathogenesis, since both caspase and calpain activation are linked to PD (Perier et al., 2012). Two studies report detection of Parkin processed to a ~41/42 kDa form in human brains of a control (Schlossmacher et al., 2002) and a PD patient (Shimura et al., 1999), but there is no discussion of the possible cleavage mechanisms.

Since cAMP-signaling is considered to be neuroprotective (Huang et al., 2013a), we tested the effects of raising intracellular cAMP levels with the lipophilic peptide PACAP27 as a potential therapeutic strategy for PD that can target Parkin. PACAP27 mitigated the loss of cell viability, caspase-3 activation, and caspase-cleavage of Parkin induced by PGJ2 in rat midbrain cultures. In contrast, calpain-cleavage of Parkin induced by Oligo, was diminished by cyclocreatine. Interestingly, cyclocreatine was used *in vivo* to improve cognition in mice with creatine transporter deficiency (Kurosawa et al., 2012), and in other neurodegenerative conditions including PD (Beal, 2011).

In conclusion, our data suggest that Parkin undergoes calcium-dependent calpain-cleavage that could potentially affect its intracellular localization and function. Phosphorylated Parkin is less sensitive to cleavage by calpain. Moreover, cleaved Parkin localizes to mitochondria in response to mitochondrial and proteasomal impairment, and the product of inflammation PGJ2. This is highly significant to PD as Parkin dysfunction is associated with familial as well as sporadic forms of PD. Recent studies underline the impact of calcium in PD-neurodegeneration, showing that C-terminal calcium binding to α-synuclein modulates synaptic vesicle interaction, and that an imbalance in calcium can cause synaptic vesicle clustering (Lautenschlager et al., 2018). Based on these studies, it was proposed that excessive levels of calcium in the brain may trigger the formation of toxic protein clumps typical of PD (Lopes, 2018). Moreover, ongoing clinical trials in PD patients are evaluating the clinical benefit of calcium channel blockers (Lopes, 2018). Since PD is associated with multifaceted pathological mechanisms, we propose that therapeutic approaches should include targeting necrosis (calpain activation) and apoptosis (caspase activation) to effectively treat (stop/delay) the progression of neurodegeneration in PD.

Supplementary Material

Refer to Web version on PubMed Central for supplementary material.

Acknowledgements:

We thank Mr. Jordy Sepulveda for his technical assistance. This work was supported by NIH [R01 AG028847 to M.E.F.-P from NIA; U54 NS041073 (SNRP) to M.E.F.-P head of sub-project from NINDS (both expired); and MD007599 to Hunter College from NIMHD], by a PSC-CUNY Research Award (ENHC-48–45 to M.E.F.-P.), and the Graduate Center Biology Program, City University of New York. We thank the MJ Fox foundation for the anti-pSer^{65}Parkin rabbit monoclonal antibody

Abbreviations:

$\Delta\Psi_m$	mitochondrial membrane potential
Ca^{++}	calcium
C3I	caspase III inhibitor (Z-DEVD-FMK)
CCr	cyclocreatine
CHO	Chinese hamster ovary
CPT	calpeptin (Z-Leu-Nle-CHO)
DMSO	dimethyl sulfoxide
ECL	enhanced chemiluminescence
Epox	epoxomicin
IBR	in between ring domain
MTT	3-(4,5-dimethylthiazol-2-yl)-2,5-diphenyl tetrazolium bromide

OA	okadaic acid
Oligo	oligomycin
PACAP	pituitary adenylate cyclase-activating peptide
PAGE	polyacrylamide gel electrophoresis
PBS	phosphate buffer saline
PD	Parkinson's disease
PGJ2 and J2	prostaglandin J2
RING	real important novel gene domain
ROS	reactive oxygen species
Rpn	regulatory particle non-ATPase
Rpt	regulatory particle triple-A ATPase
SDS	sodium dodecyl sulfate
s.e.	standard error
Suc-LLVY-AMC	succinyl-Leu-Leu-Val-Tyr-7-amino-4-methylcoumarin
Tom20	translocase of the outer membrane
Ub	ubiquitin
Ub-conjugate	ubiquitin conjugate
UbLD	ubiquitin like domain
UPP	ubiquitin/proteasome pathway
VDAC	voltage-dependent anion channel
VTA	ventral tegmental area

Reference List

Altieri DC (2013) Hsp90 regulation of mitochondrial protein folding: from organelle integrity to cellular homeostasis. Cell Mol Life Sci 70:2463–2472. [PubMed: 23052217]

Beal MF (2011) Neuroprotective effects of creatine. Amino Acids 40:1305–1313. [PubMed: 21448659]

Becker C, Jick SS, Meier CR (2010) Risk of stroke in patients with idiopathic Parkinson disease. Parkinsonism Relat Disord 16:31–35. [PubMed: 19640771]

Betarbet R, Sherer TB, MacKenzie G, Garcia-Osuna M, Panov AV, Greenamyre JT (2000) Chronic systemic pesticide exposure reproduces features of Parkinson's disease. Nat Neurosci 3:1301–1306. [PubMed: 11100151]

Bose S, Weikl T, Bugl H, Buchner J (1996) Chaperone function of Hsp90-associated proteins. Science 274:1715–1717. [PubMed: 8939863]

Boudreau RT, Hoskin DW (2005) The use of okadaic acid to elucidate the intracellular role(s) of protein phosphatase 2A: lessons from the mast cell model system. Int Immunopharmacol 5:1507–1518. [PubMed: 16023602]

Brewer GJ, Torricelli JR, Evege EK, Price PJ (1993) Optimized survival of hippocampal neurons in B27-supplemented Neurobasal, a new serum-free medium combination. J Neurosci Res 35:567–576. [PubMed: 8377226]

Brini M, Carafoli E (2011) The plasma membrane Ca(2)+ ATPase and the plasma membrane sodium calcium exchanger cooperate in the regulation of cell calcium. Cold Spring Harb Perspect Biol 3:a004168. [PubMed: 21421919]

Burke JF, Stulc JL, Skolarus LE, Sears ED, Zahuranec DB, Morgenstern LB (2013) Traumatic brain injury may be an independent risk factor for stroke. Neurology 81:33–39. [PubMed: 23803315]

Byrd RA, Weissman AM (2013) Compact Parkin only: insights into the structure of an autoinhibited ubiquitin ligase. EMBO J 32:1504–2516.

Cali T, Ottolini D, Brini M (2014) Calcium signaling in Parkinson's disease. Cell Tissue Res 357:439–454. [PubMed: 24781149]

Chan CS, Gertler TS, Surmeier DJ (2009) Calcium homeostasis, selective vulnerability and Parkinson's disease. Trends Neurosci 32:249–256. [PubMed: 19307031]

Chua BT, Guo K, Li P (2000) Direct cleavage by the calcium-activated protease calpain can lead to inactivation of caspases. J Biol Chem 275:5131–5135. [PubMed: 10671558]

Corwin C, Nikolopoulou A, Pan AL, Nunez-Santos M, Vallabhajosula S, Serrano P, Babich J, Figueiredo-Pereira ME (2018) Prostaglandin D2/J2 signaling pathway in a rat model of neuroinflammation displaying progressive parkinsonian-like pathology: potential novel therapeutic targets. J Neuroinflammation 15:272. [PubMed: 30236122]

Dagata V, Cavallaro S (2004) Parkin transcript variants in rat and human brain. Neurochem Res 29:1715–1724. [PubMed: 15453267]

Dauer W, Przedborski S (2003) Parkinson's disease: mechanisms and models. Neuron 39:889–909. [PubMed: 12971891]

Dawson TM, Dawson VL (2010) The role of parkin in familial and sporadic Parkinson's disease. Mov Disord 25 Suppl 1:S32–S39. [PubMed: 20187240]

Dedkova EN, Sigova AA, Zinchenko VP (2000) Mechanism of action of calcium ionophores on intact cells: ionophore-resistant cells. Membr Cell Biol 13:357–368. [PubMed: 10768486]

Degli EM (1998) Inhibitors of NADH-ubiquinone reductase: an overview. Biochim Biophys Acta 1364:222–235. [PubMed: 9593904]

Dufty BM, Warner LR, Hou ST, Jiang SX, Gomez-Isla T, Leenhouts KM, Oxford JT, Feany MB, Masliah E, Rohn TT (2007) Calpain-cleavage of alpha-synuclein: connecting proteolytic processing to disease-linked aggregation. Am J Pathol 170:1725–1738. [PubMed: 17456777]

DuVerle DA, Ono Y, Sorimachi H, Mamitsuka H (2011) Calpain cleavage prediction using multiple kernel learning. PLoS ONE 6:e19035. [PubMed: 21559271]

Ellington WR (2001) Evolution and physiological roles of phosphagen systems. Annu Rev Physiol 63:289–325. [PubMed: 11181958]

Endo A, Matsumoto M, Inada T, Yamamoto A, Nakayama KI, Kitamura N, Komada M (2009) Nucleolar structure and function are regulated by the deubiquitylating enzyme USP36. J Cell Sci 122:678–686. [PubMed: 19208757]

Exner N, Lutz AK, Haass C, Winklhofer KF (2012) Mitochondrial dysfunction in Parkinson's disease: molecular mechanisms and pathophysiological consequences. EMBO J 31:3038–3062. [PubMed: 22735187]

Figueiredo-Pereira ME, Rockwell P, Schmidt-Glenewinkel T, Serrano P (2015) Neuroinflammation and J2 prostaglandins: linking impairment of the ubiquitin-proteasome pathway and mitochondria to neurodegeneration. Frontiers in Mol Neurosci 7:104.

Goffredo D, Rigamonti D, Tartari M, De MA, Verderio C, Matteoli M, Zuccato C, Cattaneo E (2002) Calcium-dependent cleavage of endogenous wild-type huntingtin in primary cortical neurons. J Biol Chem 277:39594–39598. [PubMed: 12200414]

Gong CX, Lidsky T, Wegiel J, Zuck L, Grundke-Iqbal I, Iqbal K (2000) Phosphorylation of microtubule-associated protein tau is regulated by protein phosphatase 2A in mammalian brain.

Implications for neurofibrillary degeneration in Alzheimer's disease. J Biol Chem 275:5535–5544. [PubMed: 10681533]

Groll M, Kim KB, Kairies N, Huber R, Crews CM (2000) Crystal structure of epoxomicin:20S proteasome reveals a molecular basis of α',β'-epoxomicin proteasome inhibitors. J Am Chem Soc 122:1237–1238.

Hachiya N, Mihara K, Suda K, Horst M, Schatz G, Lithgow T (1995) Reconstitution of the initial steps of mitochondrial protein import. Nature 376:705–709. [PubMed: 7651521]

Ham SJ, Lee SY, Song S, Chung JR, Choi S, Chung J (2016) Interaction between RING1 (R1) and the Ubiquitin-like (UBL) Domains Is Critical for the Regulation of Parkin Activity. J Biol Chem 291:1803–1816. [PubMed: 26631732]

Harmar AJ, Fahrenkrug J, Gozes I, Laburthe M, May V, Pisegna JR, Vaudry D, Vaudry H, Waschek JA, Said SI (2012) Pharmacology and functions of receptors for vasoactive intestinal peptide and pituitary adenylate cyclase-activating polypeptide: IUPHAR review 1. Br J Pharmacol 166:4–17. [PubMed: 22289055]

Hauser DN, Hastings TG (2013) Mitochondrial dysfunction and oxidative stress in Parkinson's disease and monogenic parkinsonism. Neurobiol Dis 51:35–42. [PubMed: 23064436]

Hickey RW, Adelson PD, Johnnides MJ, Davis DS, Yu Z, Rose ME, Chang YF, Graham SH (2007) Cyclooxygenase-2 activity following traumatic brain injury in the developing rat. Pediatr Res 62:271–276. [PubMed: 17622965]

Hsieh CH, Shaltouki A, Gonzalez AE, Bettencourt da CA, Burbulla LF, St LE, Schule B, Krainc D, Palmer TD, Wang X (2016) Functional Impairment in Miro Degradation and Mitophagy Is a Shared Feature in Familial and Sporadic Parkinson's Disease. Cell Stem Cell 19:709–724. [PubMed: 27618216]

Huang H, Wang H, Figueiredo-Pereira ME (2013a) Regulating the Ubiquitin/Proteasome Pathway Via cAMP-signaling: Neuroprotective Potential. Cell Biochem Biophys 67:55–66. [PubMed: 23686612]

Huang Q, Wang H, Perry SW, Figueiredo-Pereira ME (2013b) Negative regulation of 26S proteasome stability via calpain-mediated cleavage of Rpn10 subunit upon mitochondrial dysfunction in neurons. J Biol Chem 288:12161–12174. [PubMed: 23508964]

Hutson CB, Lazo CR, Mortazavi F, Giza CC, Hovda D, Chesselet MF (2011) Traumatic brain injury in adult rats causes progressive nigrostriatal dopaminergic cell loss and enhanced vulnerability to the pesticide paraquat. J Neurotrauma 28:1783–1801. [PubMed: 21644813]

Joselin AP, Hewitt SJ, Callaghan SM, Kim RH, Chung YH, Mak TW, Shen J, Slack RS, Park DS (2012) ROS-dependent regulation of Parkin and DJ-1 localization during oxidative stress in neurons. Hum Mol Genet 21:4888–4903. [PubMed: 22872702]

Kahns S, Lykkebo S, Jakobsen LD, Nielsen MS, Jensen PH (2002) Caspase-mediated parkin cleavage in apoptotic cell death. J Biol Chem 277:15303–15308. [PubMed: 11839750]

Kao SY (2009) DNA damage induces nuclear translocation of parkin. J Biomed Sci 16:67. [PubMed: 19615059]

Kar P, Samanta K, Shaikh S, Chowdhury A, Chakraborti T, Chakraborti S (2010) Mitochondrial calpain system: an overview. Arch Biochem Biophys 495:1–7. [PubMed: 20035707]

Kazlauskaite A, Martinez-Torres RJ, Wilkie S, Kumar A, Peltier J, Gonzalez A, Johnson C, Zhang J, Hope AG, Peggie M, Trost M, van Aalten DM, Alessi DR, Prescott AR, Knebel A, Walden H, Muqit MM (2015) Binding to serine 65-phosphorylated ubiquitin primes Parkin for optimal PINK1-dependent phosphorylation and activation. EMBO Rep 16:939–954. [PubMed: 26116755]

Kondapalli C, Kazlauskaite A, Zhang N, Woodroof HI, Campbell DG, Gourlay R, Burchell L, Walden H, Macartney TJ, Deak M, Knebel A, Alessi DR, Muqit MM (2012) PINK1 is activated by mitochondrial membrane potential depolarization and stimulates Parkin E3 ligase activity by phosphorylating Serine 65. Open Biol 2:120080. [PubMed: 22724072]

Kondo M, Shibata T, Kumagai T, Osawa T, Shibata N, Kobayashi M, Sasaki S, Iwata M, Noguchi N, Uchida K (2002) 15-Deoxy-Delta(12,14)-prostaglandin J(2): the endogenous electrophile that induces neuronal apoptosis. Proc Natl Acad Sci U S A 99:7367–7372. [PubMed: 12032289]

Kumar P, Pradhan K, Karunya R, Ambasta RK, Querfurth HW (2012) Cross-functional E3 ligases Parkin and C-terminus Hsp70-interacting protein in neurodegenerative disorders. J Neurochem 120:350–370. [PubMed: 22098618]

Kunz T, Marklund N, Hillered L, Oliw EH (2002) Cyclooxygenase-2, prostaglandin synthases, and prostaglandin H2 metabolism in traumatic brain injury in the rat. J Neurotrauma 19:1051–1064. [PubMed: 12482118]

Kurosawa Y, Degrauw TJ, Lindquist DM, Blanco VM, Pyne-Geithman GJ, Daikoku T, Chambers JB, Benoit SC, Clark JF (2012) Cyclocreatine treatment improves cognition in mice with creatine transporter deficiency. J Clin Invest 122:2837–2846. [PubMed: 22751104]

Lauckner J, Frey P, Geula C (2003) Comparative distribution of tau phosphorylated at Ser262 in pre-tangles and tangles. Neurobiol Aging 24:767–776. [PubMed: 12927759]

Lautenschlager J, Stephens AD, Fusco G, Strohl F, Curry N, Zacharopoulou M, Michel CH, Laine R, Nespovitaya N, Fantham M, Pinotsi D, Zago W, Fraser P, Tandon A, St George-Hyslop P, Rees E, Phillips JJ, De SA, Kaminski CF, Schierle GSK (2018) C-terminal calcium binding of alpha-synuclein modulates synaptic vesicle interaction. Nat Commun 9:712. [PubMed: 29459792]

Liu H, Li W, Ahmad M, Miller TM, Rose ME, Poloyac SM, Uechi G, Balasubramani M, Hickey RW, Graham SH (2011a) Modification of ubiquitin-C-terminal hydrolase-L1 by cyclopentenone prostaglandins exacerbates hypoxic injury. Neurobiol Dis 41:318–328. [PubMed: 20933087]

Liu H, Li W, Ahmad M, Rose ME, Miller TM, Yu M, Chen J, Pascoe JL, Poloyac SM, Hickey RW, Graham SH (2013) Increased generation of cyclopentenone prostaglandins after brain ischemia and their role in aggregation of ubiquitinated proteins in neurons. Neurotox Res 24:191–204. [PubMed: 23355003]

Liu Y, Schubert DR (2009) The specificity of neuroprotection by antioxidants. J Biomed Sci 16:98. [PubMed: 19891782]

Liu Z, Cao J, Gao X, Ma Q, Ren J, Xue Y (2011b) GPS-CCD: a novel computational program for the prediction of calpain cleavage sites. PLoS ONE 6:e19001. [PubMed: 21533053]

Lopes JM (2018) Excessive Calcium Levels in Brain May Play Role in Parkinson's Disease

Meng L, Mohan R, Kwok BH, Elofsson M, Sin N, Crews CM (1999) Epoxomicin, a potent and selective proteasome inhibitor, exhibits in vivo antiinflammatory activity. Proc Natl Acad Sci U S A 96:10403–10408. [PubMed: 10468620]

Mengesdorf T, Jensen PH, Mies G, Aufenberg C, Paschen W (2002) Down-regulation of parkin protein in transient focal cerebral ischemia: A link between stroke and degenerative disease? Proc Natl Acad Sci U S A 99:15042–15047. [PubMed: 12415119]

Metcalfe MJ, Huang Q, Figueiredo-Pereira ME (2012) Coordination between proteasome impairment and caspase activation leading to TAU pathology: neuroprotection by cAMP. Cell Death Dis 3:e326. [PubMed: 22717581]

Migliore L, Scarpato R, Coppede F, Petrozzi L, Bonuccelli U, Rodilla V (2001) Chromosome and oxidative damage biomarkers in lymphocytes of Parkinson's disease patients. Int J Hyg Environ Health 204:61–66. [PubMed: 11725348]

Mizuno Y, Asakawa S, Suzuki T, Hattori N, Minoshima S, Chiba T, Yoshino H, Shimizu N, Tanaka K (2003) Parkin mutations. In: Genetics of movement disorders (Pulst S-M, ed), pp 305–314. San Diego: Elsevier Science.

Myeku N, Metcalfe MJ, Huang Q, Figueiredo-Pereira M (2011) Assessment of proteasome impairment and accumulation/aggregation of ubiquitinated proteins in neuronal cultures. Methods Mol Biol 793:273–296. [PubMed: 21913107]

Nam Y, Brewer GJ, Wheeler BC (2007) Development of astroglial cells in patterned neuronal cultures. J Biomater Sci Polym Ed 18:1091–1100. [PubMed: 17706000]

Oddo S (2008) The ubiquitin-proteasome system in Alzheimer's disease. J Cell Mol Med 12:363–373. [PubMed: 18266959]

Orrenius S, Zhivotovsky B, Nicotera P (2003) Regulation of cell death: the calcium-apoptosis link. Nat Rev Mol Cell Biol 4:552–565. [PubMed: 12838338]

Park HM, Kim GY, Nam MK, Seong GH, Han C, Chung KC, Kang S, Rhim H (2009) The serine protease HtrA2/Omi cleaves Parkin and irreversibly inactivates its E3 ubiquitin ligase activity. Biochem Biophys Res Commun 387:537–542. [PubMed: 19631192]

Perier C, Bove J, Vila M (2012) Mitochondria and programmed cell death in Parkinson's disease: apoptosis and beyond. Antioxid Redox Signal 16:883–895. [PubMed: 21619488]

Petrozzi L, Lucetti C, Gambaccini G, Bernardini S, Del DP, Migliore L, Scarpato R, Bonuccelli U (2001) Cytogenetic analysis oxidative damage in lymphocytes of Parkinson's disease patients. Neurol Sci 22:83–84. [PubMed: 11487213]

Pierre SR, Lemmens MA, Figueiredo-Pereira ME (2009) Subchronic infusion of the product of inflammation prostaglandin J2 models sporadic Parkinson's disease in mice. J Neuroinflammation 6:18. [PubMed: 19630993]

Rayport S, Sulzer D, Shi WX, Sawasdikosol S, Monaco J, Batson D, Rajendran G (1992) Identified postnatal mesolimbic dopamine neurons in culture: morphology and electrophysiology. J Neurosci 12:4264–4280. [PubMed: 1359033]

Reglodi D, Kiss P, Lubics A, Tamas A (2011) Review on the protective effects of PACAP in models of neurodegenerative diseases in vitro and in vivo. Curr Pharm Des 17:962–972. [PubMed: 21524257]

Riley BE, Lougheed JC, Callaway K, Velasquez M, Brecht E, Nguyen L, Shaler T, Walker D, Yang Y, Regnstrom K, Diep L, Zhang Z, Chiou S, Bova M, Artis DR, Yao N, Baker J, Yednock T, Johnston JA (2013) Structure and function of Parkin E3 ubiquitin ligase reveals aspects of RING and HECT ligases. Nat Commun 4:1982. [PubMed: 23770887]

Rivero-Rios P, Gomez-Suaga P, Fdez E, Hilfiker S (2014) Upstream deregulation of calcium signaling in Parkinson's disease. Front Mol Neurosci 7:53. [PubMed: 24987329]

Rodriguez-Grande B, Blackabey V, Gittens B, Pinteaux E, Denes A (2013) Loss of substance P and inflammation precede delayed neurodegeneration in the substantia nigra after cerebral ischemia. Brain Behav Immun 29:51–61. [PubMed: 23232501]

Sakata E, Yamaguchi Y, Kurimoto E, Kikuchi J, Yokoyama S, Yamada S, Kawahara H, Yokosawa H, Hattori N, Mizuno Y, Tanaka K, Kato K (2003) Parkin binds the Rpn10 subunit of 26S proteasomes through its ubiquitin-like domain. EMBO Rep 4:301–306. [PubMed: 12634850]

Schapira AH (2013) Calcium dysregulation in Parkinson's disease. Brain 136:2015–2016. [PubMed: 23788521]

Schlossmacher MG, Frosch MP, Gai WP, Medina M, Sharma N, Forno L, Ochiishi T, Shimura H, Sharon R, Hattori N, Langston JW, Mizuno Y, Hyman BT, Selkoe DJ, Kosik KS (2002) Parkin localizes to the Lewy bodies of Parkinson disease and dementia with Lewy bodies. Am J Pathol 160:1655–1667. [PubMed: 12000718]

Shaik JS, Miller TM, Graham SH, Manole MD, Poloyac SM (2014) Rapid and simultaneous quantitation of prostanoids by UPLC-MS/MS in rat brain. J Chromatogr B Analyt Technol Biomed Life Sci 945–946:207–216.

Shiba-Fukushima K, Imai Y, Yoshida S, Ishihama Y, Kanao T, Sato S, Hattori N (2012) PINK1-mediated phosphorylation of the Parkin ubiquitin-like domain primes mitochondrial translocation of Parkin and regulates mitophagy. Sci Rep 2:1002. [PubMed: 23256036]

Shimura H, Hattori N, Kubo S, Yoshikawa M, Kitada T, Matsumine H, Asakawa S, Minoshima S, Yamamura Y, Shimizu N, Mizuno Y (1999) Immunohistochemical and subcellular localization of Parkin protein: absence of protein in autosomal recessive juvenile parkinsonism patients. Ann Neurol 45:668–672. [PubMed: 10319893]

Shivers KY, Nikolopoulou A, Machlovi SI, Vallabhajosula S, Figueiredo-Pereira ME (2014) PACAP27 prevents Parkinson-like neuronal loss and motor deficits but not microglia activation induced by prostaglandin J2. Biochim Biophys Acta 1842:1707–1719. [PubMed: 24970746]

Shoshan-Barmatz V, De P,V, Zweckstetter M, Raviv Z, Keinan N, Arbel N (2010) VDAC, a multi-functional mitochondrial protein regulating cell life and death. Mol Aspects Med 31:227–285. [PubMed: 20346371]

Sorimachi H, Ono Y (2012) Regulation and physiological roles of the calpain system in muscular disorders. Cardiovasc Res 96:11–22. [PubMed: 22542715]

Surmeier DJ, Schumacker PT, Guzman JD, Ilijic E, Yang B, Zampese E (2017) Calcium and Parkinson's disease. Biochem Biophys Res Commun 483:1013–1019. [PubMed: 27590583]

Surmeier DJ, Sulzer D (2013) The pathology roadmap in Parkinson disease. Prion 7:85–91. [PubMed: 23324593]

Trempe JF, Sauve V, Grenier K, Seirafi M, Tang MY, Menade M, Al-Abdul-Wahid S, Krett J, Wong K, Kozlov G, Nagar B, Fon EA, Gehring K (2013) Structure of parkin reveals mechanisms for ubiquitin ligase activation. Science 340:1451–1455. [PubMed: 23661642]

Uchida H, Yokoyama H, Kimoto H, Kato H, Araki T (2010) Long-term changes in the ipsilateral substantia nigra after transient focal cerebral ischaemia in rats. Int J Exp Pathol 91:256–266. [PubMed: 20353427]

Uchida K, Shibata T (2008) 15-Deoxy-Δ(12,14)-prostaglandin J2: an electrophilic trigger of cellular responses. Chem Res Toxicol 21:138–144. [PubMed: 18052108]

Um JW, Im E, Lee HJ, Min B, Yoo L, Yoo J, Lubbert H, Stichel-Gunkel C, Cho HS, Yoon JB, Chung KC (2010) Parkin directly modulates 26S proteasome activity. J Neurosci 30:11805–11814. [PubMed: 20810900]

Van L,V, Arnold B, Cassady SJ, Chu CT, Burton EA, Berman SB (2011) Bioenergetics of neurons inhibit the translocation response of Parkin following rapid mitochondrial depolarization. Hum Mol Genet 20:927–940. [PubMed: 21147754]

Vande WL, Lamkanfi M, Vandenabeele P (2008) The mitochondrial serine protease HtrA2/Omi: an overview. Cell Death Differ 15:453–460. [PubMed: 18174901]

Wauer T, Komander D (2013) Structure of the human Parkin ligase domain in an autoinhibited state. EMBO J 32:2099–2112. [PubMed: 23727886]

Yamamoto A, Friedlein A, Imai Y, Takahashi R, Kahle PJ, Haass C (2005) Parkin phosphorylation and modulation of its E3 ubiquitin ligase activity. J Biol Chem 280:3390–3399. [PubMed: 15557340]

Zaichick SV, McGrath KM, Caraveo G (2017) The role of Ca(2+) signaling in Parkinson's disease. Dis Model Mech 10:519–535. [PubMed: 28468938]

Mosmann T, Rapid colorimetric assay for cellular growth and survival: application to proliferation and cytotoxicity assays, J. Immunol. Methods 65 (1-2), 1983, 55–63. [PubMed: 6606682]

Highlights

- Mitochondrial failure induces Parkin cleavage by calpain in rat CNS neurons
- Calpain-cleaved Parkin is enriched in neuronal mitochondrial fractions
- Phosphatase inhibition stabilizes phosphoSer^{65}Parkin reducing its calpain-cleavage
- Calcium dyshomeostasis also induces calpain cleavage of endogenous neuronal Parkin
- Computational analysis predicts that calpain cleavage removes Parkin's UbL domain

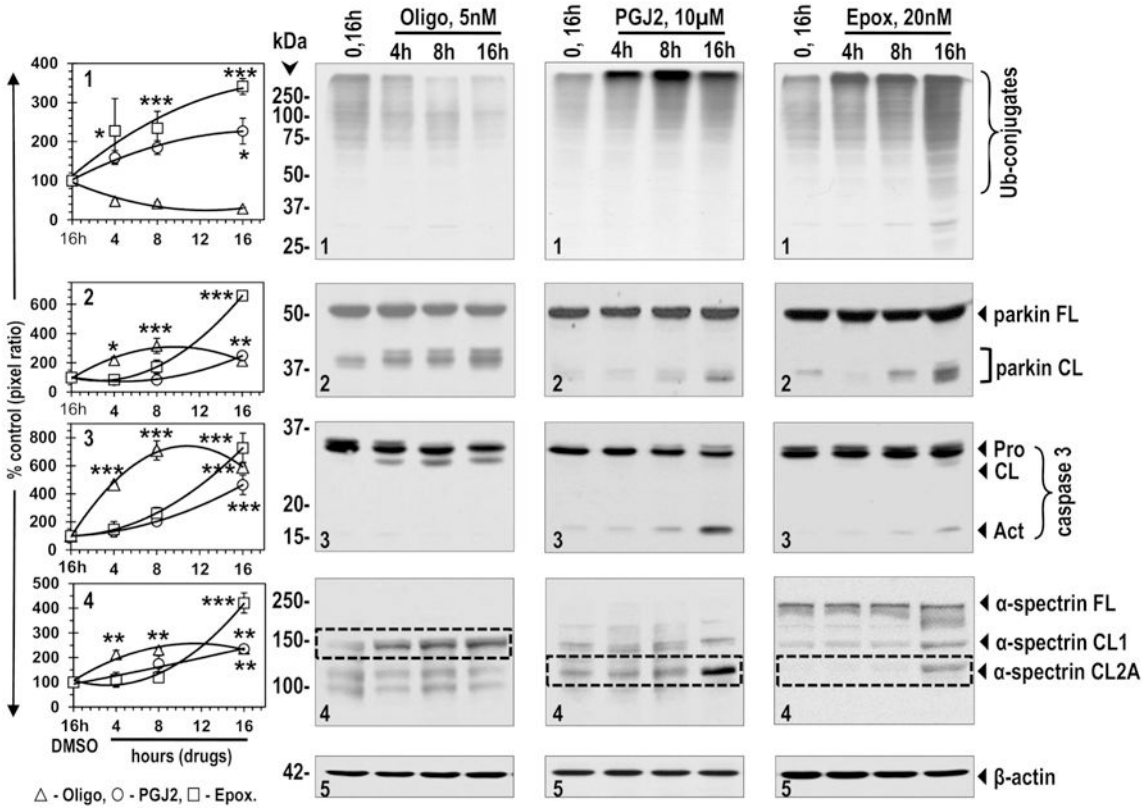

FIGURE 1. Effects of oligomycin (Oligo), prostaglandin J2 (PGJ2), and epoxomicin (Epox) on ubiquitinated proteins, and on Parkin, caspase-3 and spectrin cleavages.

Rat midbrain neuronal cultures were treated as indicated. Total lysates were analyzed by western blotting (50 μg of protein/lane) probed with the respective antibodies to detect: Ub-proteins (panels 1); full-length (FL) and cleaved (CL) Parkin (panels 2); full-length (Pro), cleaved inactive (CL), and cleaved active (Act) caspase-3 (panels 3); full-length (FL), calpain-cleaved (CL1) and caspase-cleaved (CL2) α-spectrin (panels 4); β-actin (loading control, panels 5). Molecular mass markers in kDa are shown on the left of the blots. Graphs (far left, polynomial order 2) show semi-quantification of the respective signals by densitometry. Data represent the percentage of the pixel ratio for Ub-proteins (1), cleaved Parkin (2), cleaved inactive (for Oligo) and cleaved active (for PGJ2 and Epox) caspase-3 (3), or calpain-cleaved (for Oligo) and caspase-cleaved (for PGJ2 and Epox) α-spectrin (4), over β-actin (5) for each condition compared to Oligo control (100%). Values are means ± s.e. from at least three experiments. Asterisks identify values that are significantly different from Oligo control (one-way ANOVA, Dunnett's multiple comparison test, *$p<0.05$, **$p<0.01$, ***$p<0.001$). Δ - Oligo, O - PGJ2, □ - Epox.

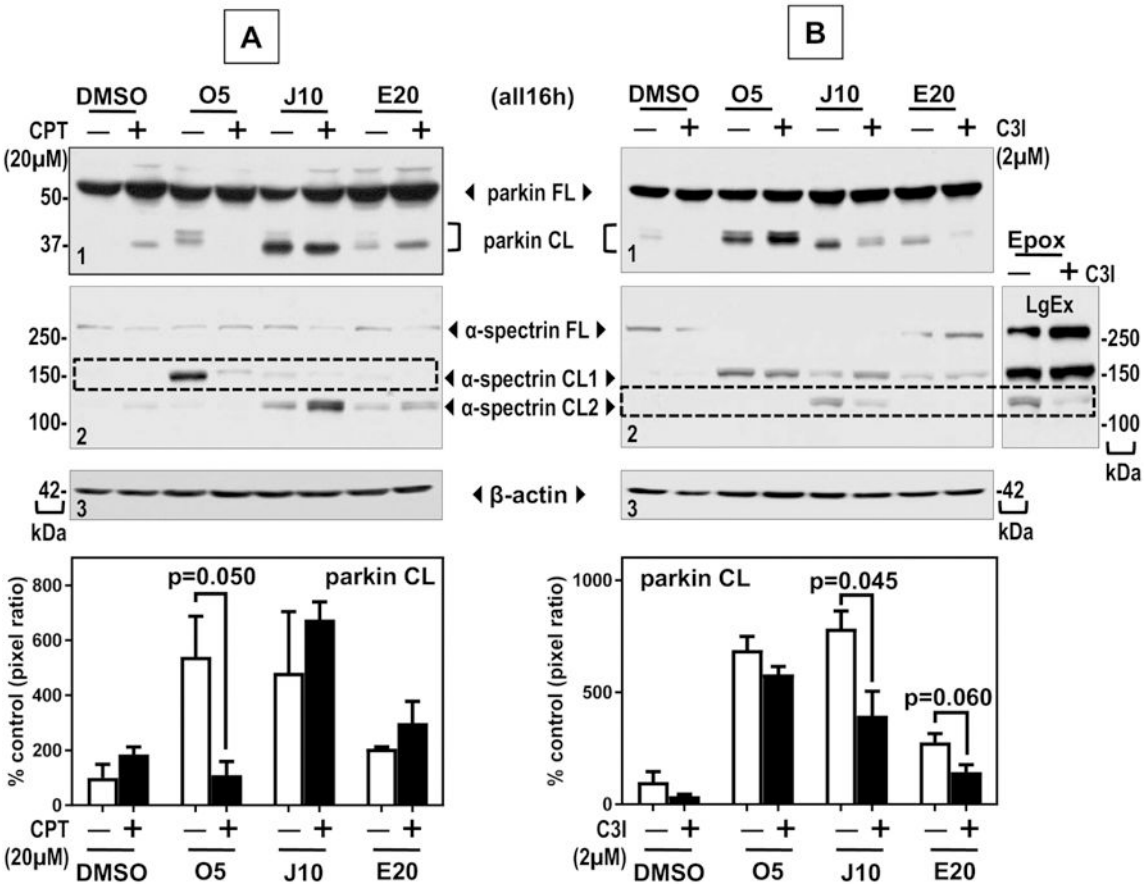

FIGURE 2. Effects of the calpain inhibitor calpeptin (A, CPT, Z-Leu-Nle-CHO) and the caspase-3 inhibitor (B, C3I, Z-DEVD-FMK) on Parkin and spectrin cleavages induced by oligomycin (O, 5nM), PGJ2 (J2, 10μM), and epoxomicin (E, 20nM).

Rat midbrain neuronal cultures were pre-treated for 30min with CPT (A) of C3I (B) and then for 16h with Oligo, PGJ2 or Epox as indicated. Total lysates were analyzed by western blotting (50 μg of protein/lane) probed with the respective antibodies to detect: full-length (FL) and cleaved (CL) Parkin (panels 1); full-length (FL), calpain-cleaved (CL1) and caspase-cleaved (CL2) α-spectrin (panels 2); β-actin (loading control, panels 3). Molecular mass markers in kDa are shown on the left (A) and right (B) of the blots. Graphs show semi-quantification of the respective signals by densitometry. Data represent the percentage of the pixel ratio for cleaved Parkin over β-actin for each condition compared to DMSO control (no inhibitor, 100%). Values are means ± s.e. from three experiments. Significant difference was assessed for each drug pair (± inhibitor, multiple t-test, Holm-Sidak method with $\alpha = 0.05$). Only P values (above brackets) close to significant difference are shown. LgEx, long exposure.

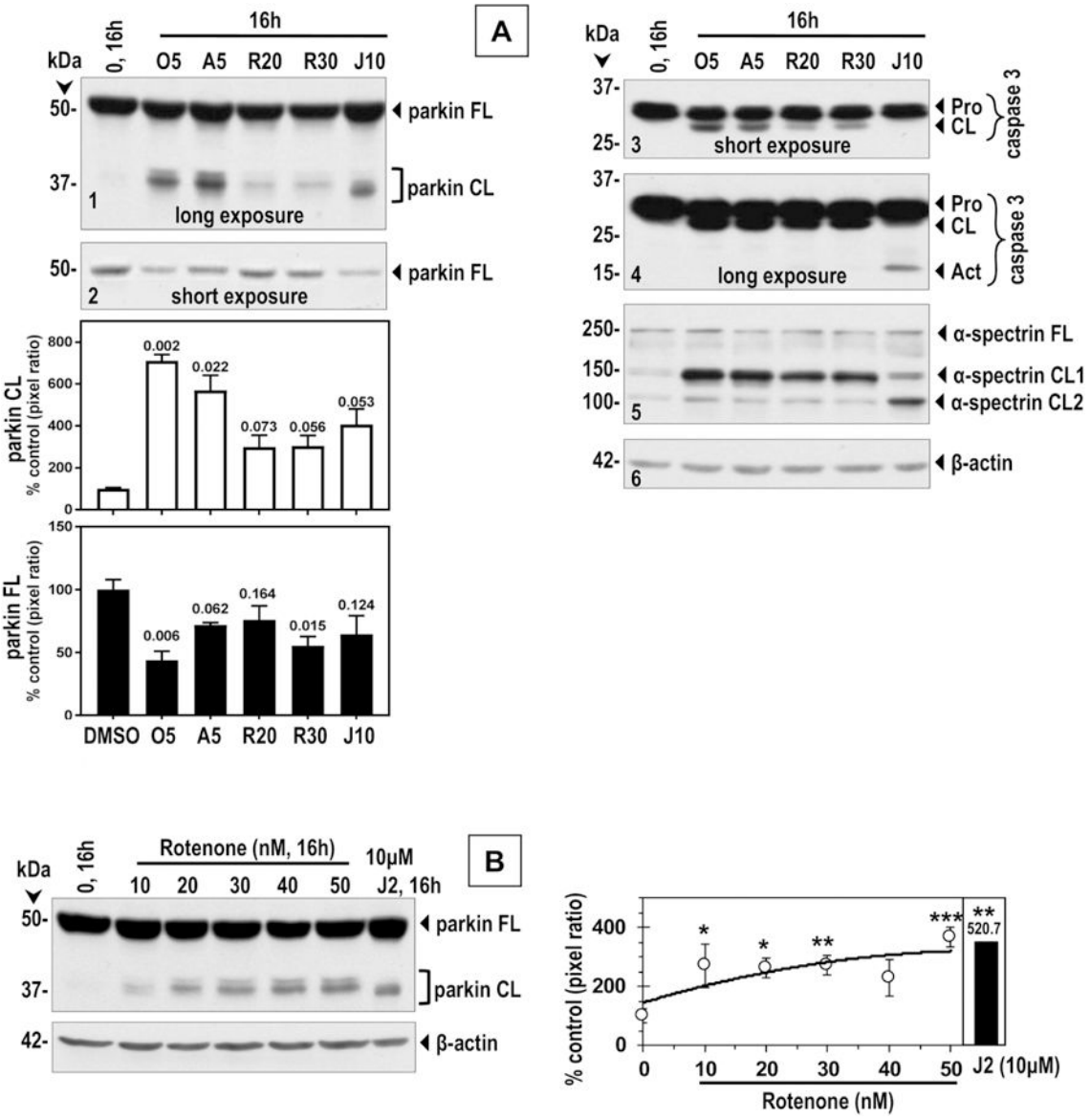

FIGURE 3. Effects of oligomycin (O, 5nM), antimycin (A, 5nM) and rotenone (R, 10nM to 50nM) on Parkin, caspase-3 and spectrin cleavages. PGJ2 (J, 10μM) is included for comparison.

Rat midbrain neuronal cultures were treated for 16h as indicated (in A and B). Total lysates were analyzed by western blotting (50 μg of protein/lane) probed with the respective antibodies to detect: full-length (FL) and cleaved (CL) Parkin (panel 1, long exposure; panel 2, short exposure); full-length (Pro), cleaved inactive (CL, panel 3, short exposure), and cleaved active (Act, panel 4, long exposure) caspase-3; full-length (FL), calpain-cleaved (CL1) and caspase-cleaved (CL2) α-spectrin (panel 5); β-actin (loading control, panel 6). Molecular mass markers in kDa are shown on the left of the blots. Graphs show semi-quantification of the respective signals by densitometry. Data represent the percentage of the pixel ratio for cleaved (CL) and full-length (FL) Parkin over β-actin for each condition compared to DMSO control (100%). (A) Values are means ± s.e. from three experiments. Respective P values shown above each bar (unpaired t test with Welch's correction). (B)

Values and means ± s.e. from three experiments. Asterisks identify values that are significantly different from control (one-way ANOVA, Dunnett's multiple comparison test, **p<0.01, ***p<0.001). O - Rotenone.

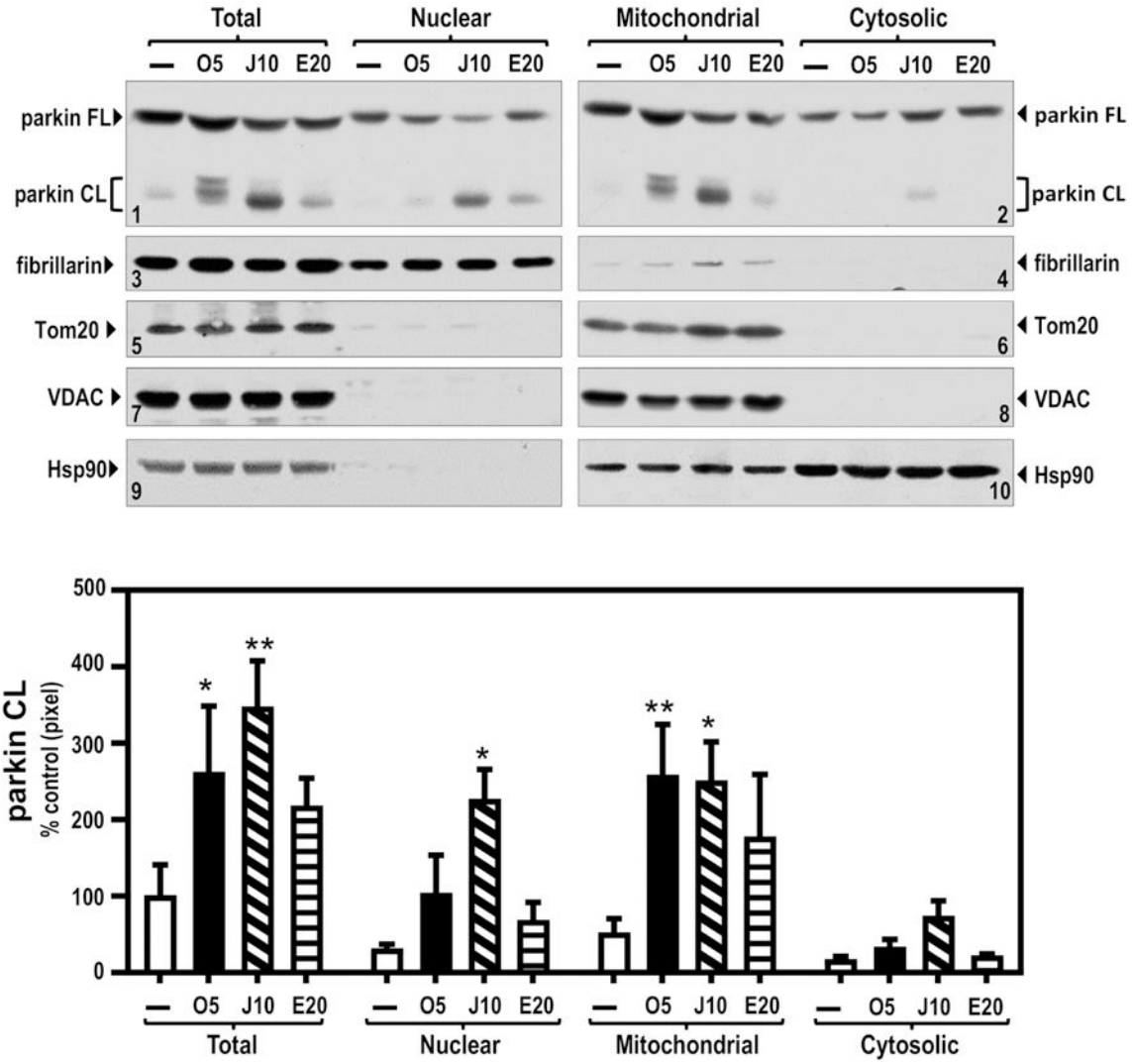

FIGURE 4. Subcellular localization of full-length (FL) and cleaved (CL) Parkin upon treatment with oligomycin (O, 5nM), PGJ2 (J2, 10μM), and epoxomicin (E, 20nM).

Ratcerebral cortical neurons were treated for 16h with Oligo, PGJ2 or Epox as indicated. Upon subcellular fractionation of the total lysates, 40 μg of protein from the total lysates, as well as nuclear, mitochondrial and cytosolic fractions were analyzed by western blotting probed for full-length (FL) and cleaved (CL) Parkin (panels 1 & 2). Subcellular fractions were validated with the following markers: nuclear (fibrillarin, panels 3 & 4), mitochondrial (Tom20, panels 5 & 6, VDAC, panels 7 & 8) and cytosolic (Hsp90, panels 9 & 10). Graphs show semi-quantification of the respective signals by densitometry. Data represent the percentage of the pixel ratio for cleaved Parkin over the respective fraction markers for each condition, compared to DMSO control (for each fraction, 100%). Values are means ± s.e. from three experiments. Asterisks identify values that are significantly different from control (two-way ANOVA with $\alpha = 0.05$, Dunnett's multiple comparison test, *$p<0.05$, **$p<0.01$).

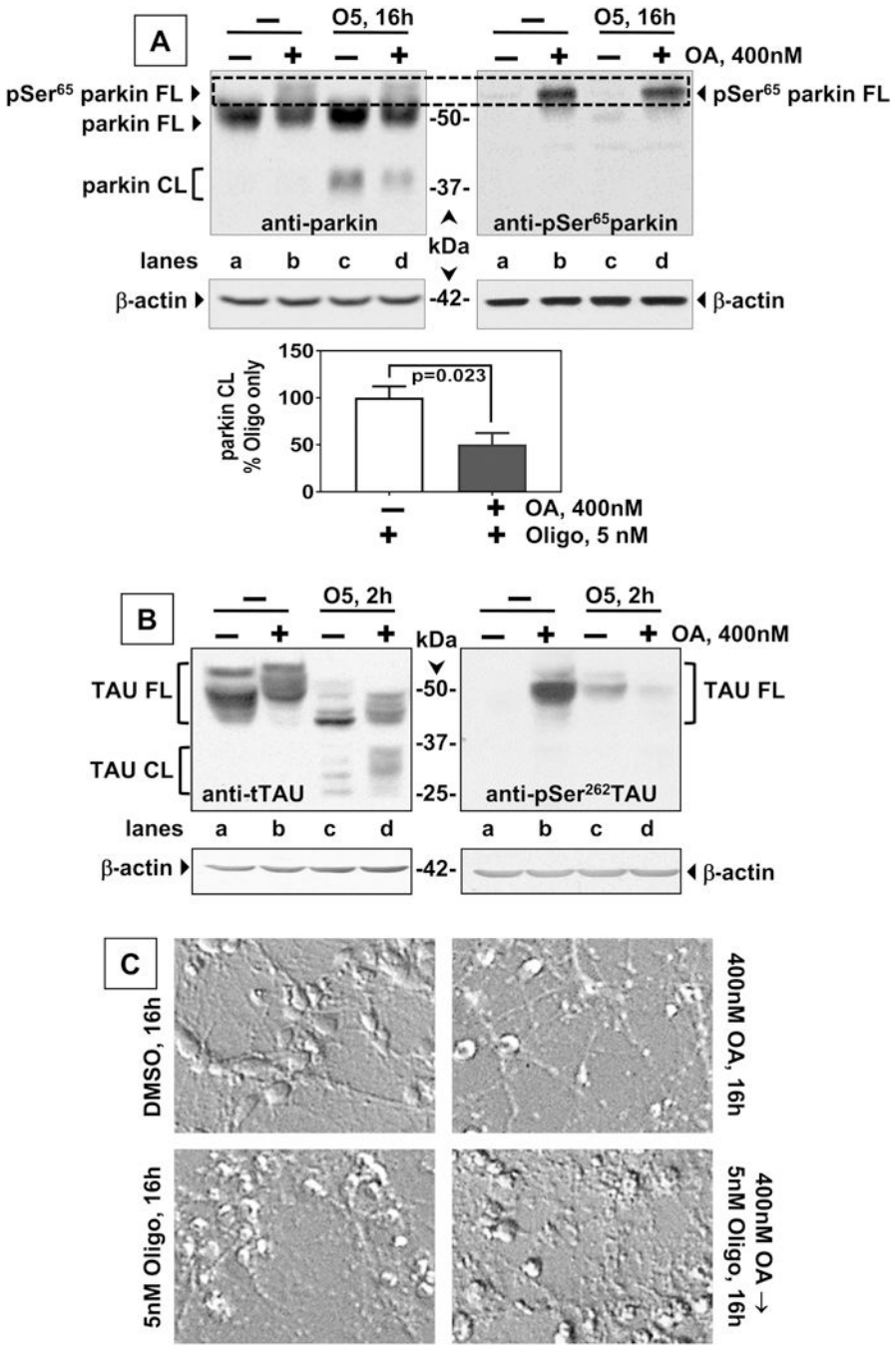

FIGURE 5. Effect of the phosphatase inhibitor okadaic acid (OA) on Parkin.

Rat cerebral cortical neurons were pre-treated for 30min with OA (400nM) and then with Oligo (O, 5nM for 16h or 2h) as indicated. Total lysates were analyzed by western blotting (50 μg of protein/lane) probed in (A) for full-length (FL) and cleaved (CL) Parkin (anti-parkin panel), parkin phosphorylated at Ser^{65} (anti-$pSer^{65}$ parkin panel), and β-actin (loading control, actin panels), and additional in (B) for total tau (tTAU) and $pSer^{262}$TAU. Molecular mass markers in kDa are shown in the middle. Full-length parkin phosphorylated at Ser^{65}, $pSer^{65}$ parkin FL. Dashed box highlights $pSer^{65}$ parkin FL. Graphs in (A) show

semi-quantification of the respective signals by densitometry. Data represent the percentage of the pixel ratio for cleaved Parkin in cells treated with OA followed by Oligo, (black bar), compared to Oligo only (white bar, 100%). Values are means ± s.e. from three experiments. The P value shows significant difference (below bracket, one tailed t-test). (C) depicts the morphology of the cortical neurons treated under the specified conditions. DIC images (20x) obtained with a LeicaDMI-4000B inverted microscope (Leica Microsystems, Buffalo Groove, IL).

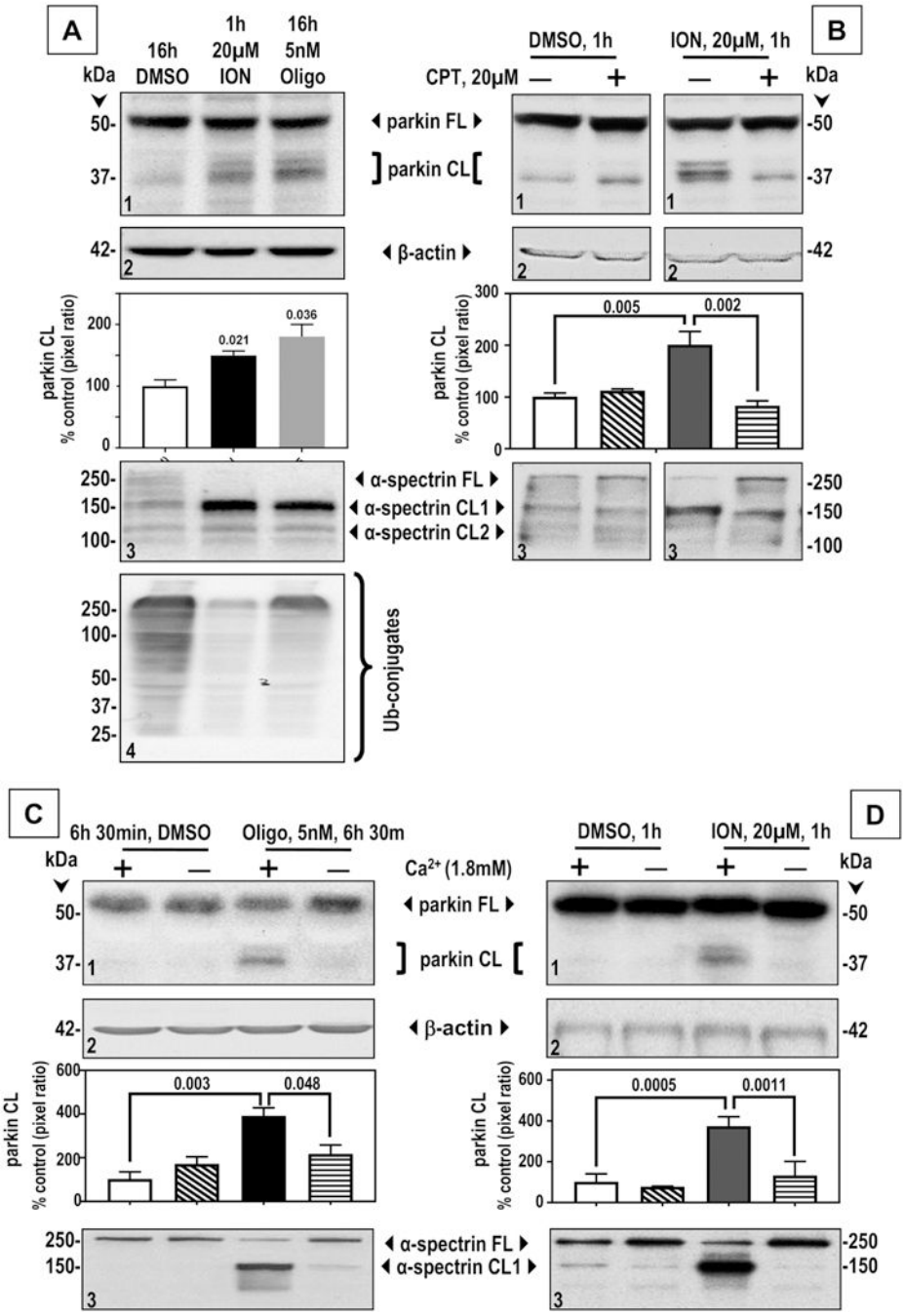

FIGURE 6. Effects of Oligo (± Ca++) and the Ca^{++} ionophore A23187 (ION, ± Ca++) on Parkin and spectrin cleavage, and on ubiquitinated protein levels.

Rat cerebral cortical neurons were treated as indicated. Total lysates were analyzed by western blotting [50 μg of protein/lane] probed with the respective antibodies to detect: full-length (FL) and cleaved (CL) Parkin (panels 1); β-actin (loading control, panels 2); full-length (FL), calpain-cleaved (CL1) and caspase-cleaved (CL2) α-spectrin (panels 3); and in (A) Ub-proteins (panel 4). In (B) cells were pre-treated for 30-min with the calpain inhibitor calpeptin (CPT, Z-Leu-Nle-CHO) prior to the Ca^{++} ionophore A23187 (1h). In (C) and (D) cells were respectively treated with Oligo (6h 30min) or A23187 (1h), in the presence and

absence of Ca^{++} (1.8mM) in the media. Molecular mass markers in kDa are shown on the right and left of the blots. Graphs show semi-quantification of the respective signals by densitometry. Data represent the percentage of the pixel ratio for cleaved (CL) Parkin over β-actin for each condition compared to DMSO control (100%). Values are means ± s.e. from three experiments for all panels. In A, the respective P values are shown above each bar (unpaired t test with Welch's correction). In B, C and D only P values close to significant difference are shown (above brackets, one-way ANOVA, Tukey's multiple comparisons test).

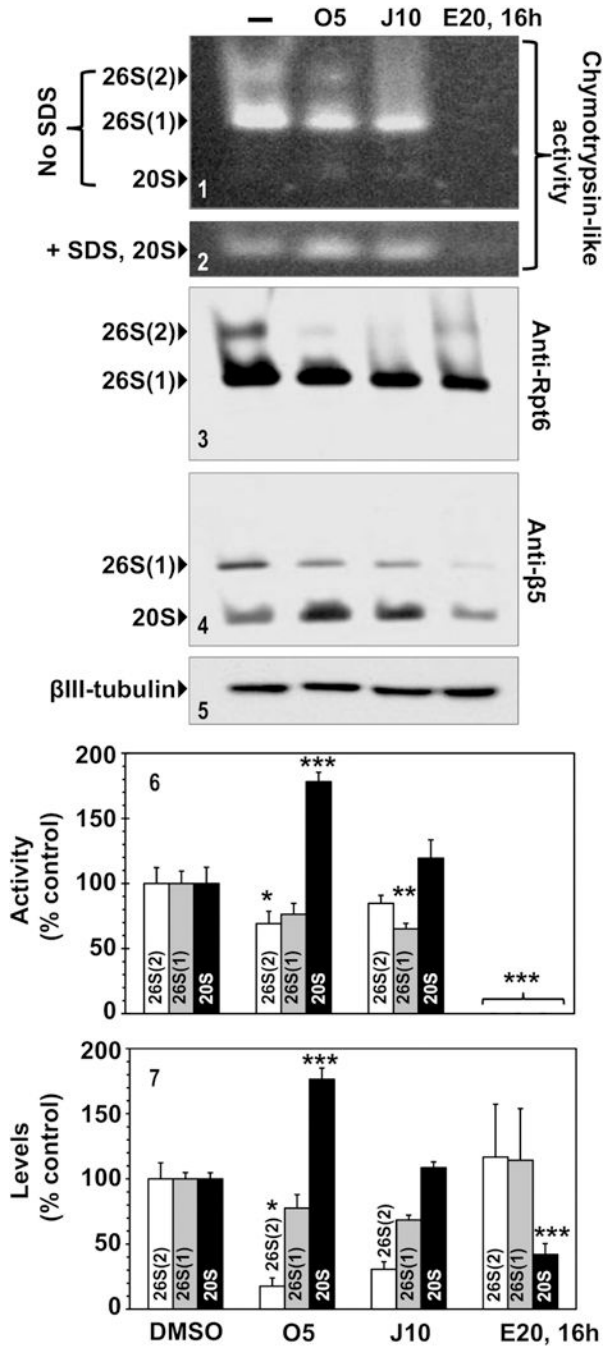

FIGURE 7. Effects of oligomycin (O, 5nM), PGJ2 (J2, 10μM), and epoxomicin (E, 20nM) on proteasome activity and levels.

Rat midbrain neuronal cultures were treated for 16h with Oligo, PGJ2, and Epox for 16h. Cleared lysates (25μg/sample) were subjected to non-denaturing gel electrophoresis as described under “Materials and Methods”. The chymotrypsin-like activity of fully assembled 26S [two caps 26S(2) and one cap 26S(1)] and 20S proteasomes (all indicated in the middle by arrows) was assessed with Suc-LLVY-AMC by the in-gel assay (panel 1). To improve detection of 20S proteasome activity, 0.04% SDS was added to the reaction buffer (panel 2). Proteasome levels were detected by immunoblotting with anti-Rpt6 (panel 3),

anti-β5 (panel 4), and anti-βIII-tubulin (panel 5, loading control) antibodies. Proteasome chymotrypsin-like activity (panel 6) and levels (panel 7) were semi-quantified by densitometry (values in graphs). Percentages represent the ratio between data for each condition and control (DMSO) considered to be 100%. Values are means ± s.e. from at least five experiments. Asterisks identify values that are significantly different from control (one-way ANOVA, Dunnett's multiple comparison test, *$p<0.05$, **$p<0.01$, ***$p<0.001$).

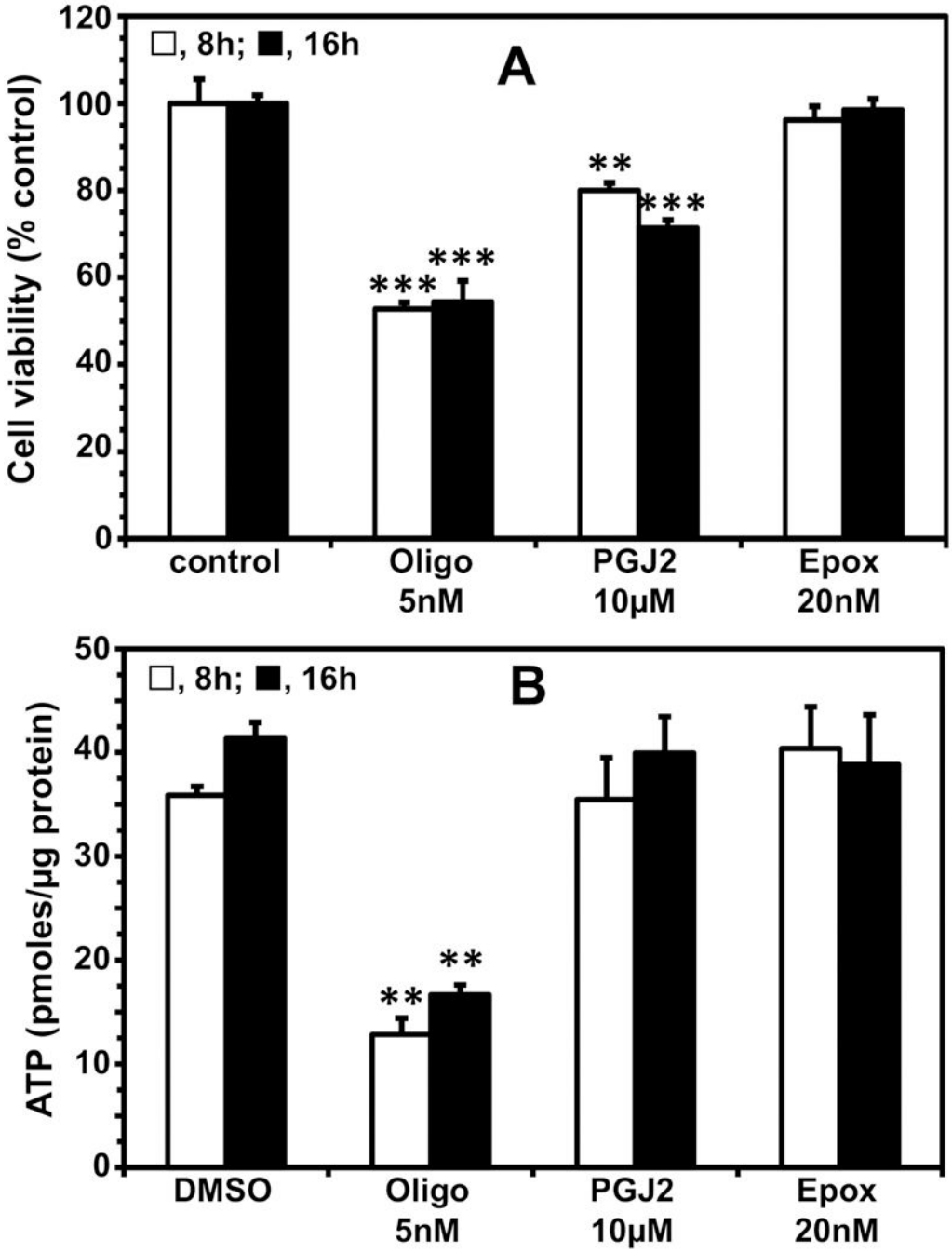

FIGURE 8. Effects of oligomycin (O, 5nM), PGJ2 (J2, 10μM), and epoxomicin (E, 20nM) on cell viability (A) and ATP levels (B).

Rat midbrain neuronal cultures were treated as indicated. Cell viability **(A)** was assessed with the MTT assay. Total **(B)** ATP steady state levels (pmoles/μg of protein) were assessed with the luciferin/luciferase system. Percentages represent the ratio between the data for each condition and control (100%). Values indicate means ± s.e. from at least three experiments per group. Asterisks identify values that are significantly different from control (one-way ANOVA, Tukey's multiple comparisons test, ** $p<0.01$; *** $p<0.001$).

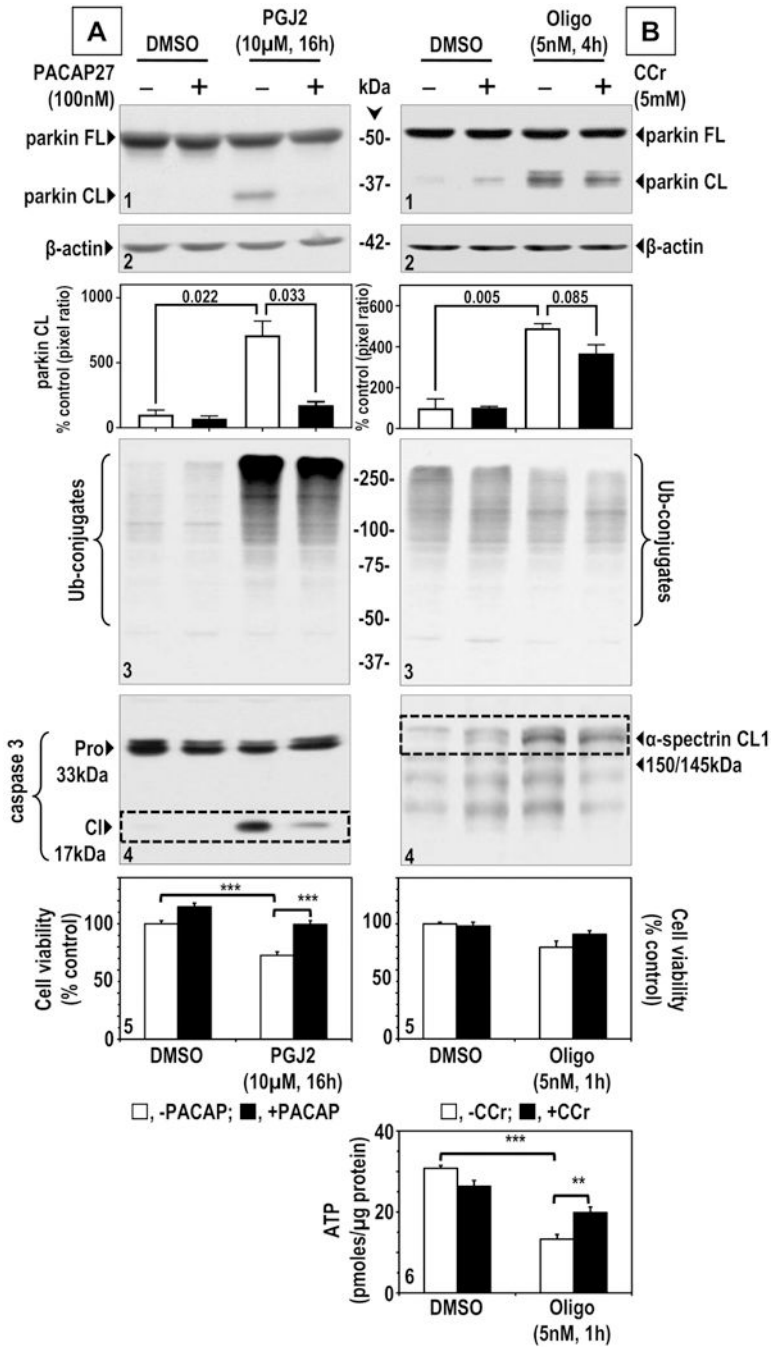

FIGURE 9. PACAP27 and cyclocreatine diminish the effects of PGJ2 or oligomycin (Oligo), respectively.

Rat midbrain cultures were treated with DMSO (control, vehicle), or: **(A)** PGJ2 (10μM, 16h) in conjunction with water (control, vehicle) or PACAP27 (100nM); in **(B)** Oligo [5nM, 1h (panels 5 & 6) or 4h (panels 1–4)] in conjunction with cyclocreatine (CCr, 5mM in medium). For the 4h Oligo treatment CCr was co-added and then added again two hours post-Oligo. Total lysates were analyzed by western blotting (50 μg of protein/lane) probed for full-length (FL) and cleaved (CL) Parkin (panels 1); β-actin (loading control, panels 2). Ub-proteins (panels 3); full-length (Pro) and cleaved active (Cl) caspase-3 (panels 4A); full-

length (FL), and calpain-cleaved (CL1) α-spectrin (panels 4B). Molecular mass markers in kDa are shown in the middle. Graphs show semi-quantification of the respective signals by densitometry. Data represent the percentage of the pixel ratio for cleaved (CL) Parkin over β-actin for each condition compared to DMSO control (100%). Values are means ± s.e. from three experiments. Relevant P values shown (above brackets, unpaired t test with Welch's correction).

Cell viability (panels 5) was assessed with the MTT assay. Percentages represent the ratio between the data for each condition and control (100%). ATP steady state levels (pmoles/μg of protein, panel 6) were measured with the luciferin/luciferase system. Values indicate means ± s.e from at least 4 determinations. Asterisks identify values that are significantly different (two-tailed t-test) as indicated, with **p<0.01, ***p<0.001.

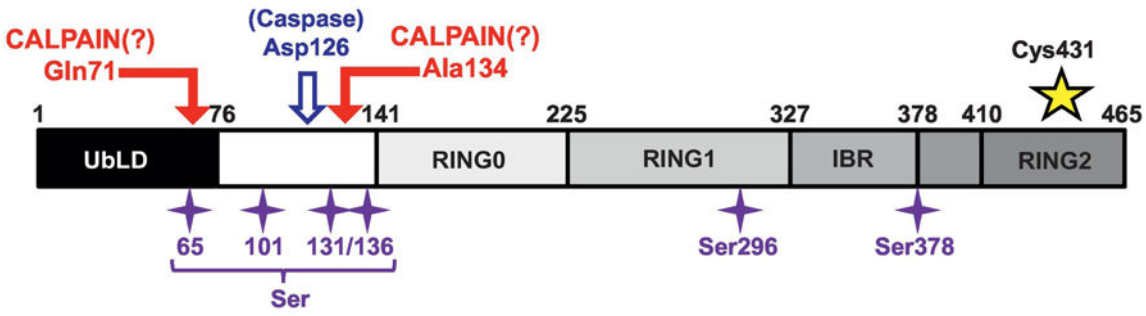

FIGURE 10 –. Model for Parkin structure and domains showing the potential calpain-mediated cleavage sites.

C431, catalytic cysteine; purple stars, Ser phosphorylation sites; Asp126, caspase-cleavage site; Gln71 and Ala134, predicted calpain cleavage sites. UbLD, ubiquitin like domain; RING, real important novel gene domains; IBR, in between ring domain. Modified from (Byrd and Weissman, 2013) and based on (Wauer and Komander, 2013;Riley et al., 2013;Trempe et al., 2013).